AD-A067 079 NAVAL ENVIRONMENTAL PREDICTION RESEARCH FACILITY MON--ETC F/G 4/2
LEVEL ASSIGNMENT IN THE ASSIMILATION OF SATELLITE CLOUD-TRACKED--ETC(U)
DEC 78 D H LEE

UNCLASSIFIED NEPRF-TR-78-03 NL

| OF |
AD
A067079

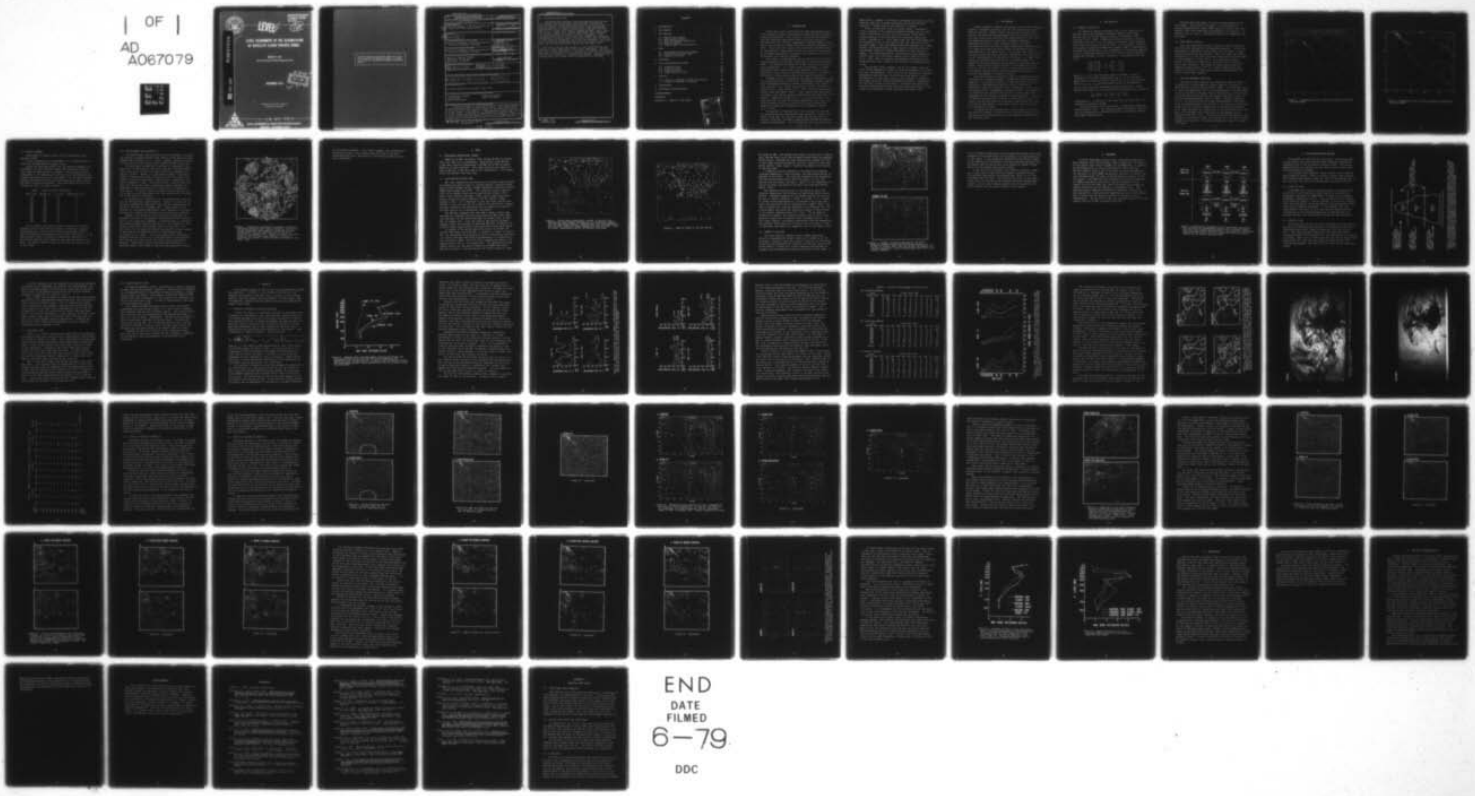

END
DATE
FILMED
6-79
DDC

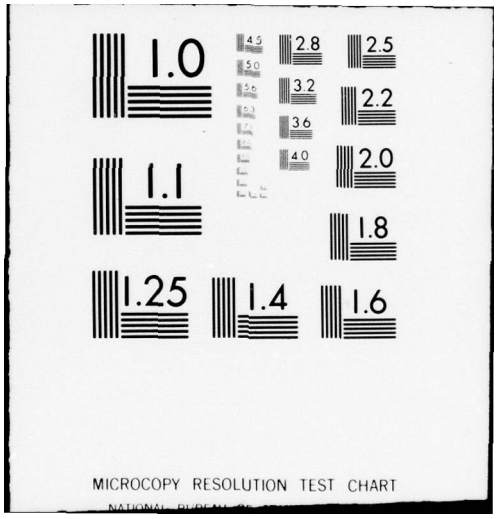
1.0
1.1
1.25
1.4
1.6
1.8
2.0
2.2
2.5
2.8
3.2
3.6
4.0
4.5
5.0
5.6
MICROCOPY RESOLUTION TEST CHART

NAVENVPREDRSCHFAC
TECHNICAL REPORT
TR 78-03

LEVEL II

12 B.S.

LEVEL ASSIGNMENT IN THE ASSIMILATION OF SATELLITE CLOUD-TRACKED WINDS

David H. Lee
Naval Environmental Prediction Research Facility

DECEMBER 1978

NAVAL ENVIRONMENTAL PREDICTION RESEARCH FACILITY
MONTEREY, CALIFORNIA 93940

UNCLASSIFIED

SECURITY CLASSIFICATION OF THIS PAGE (When Data Entered)

REPORT DOCUMENTATION PAGE

READ INSTRUCTIONS BEFORE COMPLETING FORM

1. REPORT NUMBER: NAVENVPREDRSCHFAC Technical Report TR 78-03
2. GOVT ACCESSION NO.
3. RECIPIENT'S CATALOG NUMBER

4. TITLE (and Subtitle): (6) Level Assignment in the Assimilation of Satellite Cloud-Tracked Winds
5. TYPE OF REPORT & PERIOD COVERED: (9) Final Repts
6. PERFORMING ORG. REPORT NUMBER

7. AUTHOR(s): (10) David H. Lee
8. CONTRACT OR GRANT NUMBER(s)

9. PERFORMING ORGANIZATION NAME AND ADDRESS: Naval Environmental Prediction Research Facility, Monterey, CA 93940
10. PROGRAM ELEMENT, PROJECT, TASK AREA & WORK UNIT NUMBERS: PE 62759N; PN WF52551792; NEPRF W.U. 6.2-12

11. CONTROLLING OFFICE NAME AND ADDRESS: Naval Environmental Prediction Research Facility, Monterey, CA 93940
12. REPORT DATE: (11) December 1978
13. NUMBER OF PAGES: 74

14. MONITORING AGENCY NAME & ADDRESS (if different from Controlling Office): Naval Air Systems Command, Department of the Navy, Washington, DC 20361
15. SECURITY CLASS. (of this report): UNCLASSIFIED
15a. DECLASSIFICATION/DOWNGRADING SCHEDULE

16. DISTRIBUTION STATEMENT (of this Report): (16) F52,551 (17) WF52551792
Approved for public release; distribution unlimited.

17. DISTRIBUTION STATEMENT (of the abstract entered in block 20, if different from Report): (14) NEPRF-TR-78-03 (15) 73 p.

18. SUPPLEMENTARY NOTES

Original manuscript received in May 1978.

19. KEY WORDS (Continue on reverse side if necessary and identify by block number)

cloud motion vectors
cloud-winds
data assimilation
objective analysis
level assignment

20. ABSTRACT (Continue on reverse side if necessary and identify by block number)

Heights assigned to wind vectors derived from geostationary satellite data cannot be determined exactly. When these vectors are assimilated into numerical models or analyses which define finite layers in the vertical, a compounding of errors may result. In this study, the method of determining the insertion level within an assimilation system is varied in an attempt to minimize these errors and study their effect on the resultant analyses.

CONT

DD FORM 1 JAN 73 1473 EDITION OF 1 NOV 65 IS OBSOLETE
S/N 0102-014-6601

UNCLASSIFIED

SECURITY CLASSIFICATION OF THIS PAGE (When Data Entered)

407 279

20. Abstract (continued)

Rawinsonde data and SMS-2 satellite-derived cloud-tracked wind vectors were assimilated using the NCAR Limited Area Multivariate Statistical Objective Analysis, with persistence as the first guess. The domains used in the study included the northwestern Pacific Ocean, Central America and most of North America, a six-hour time interval between analyses, and a three-day period. Except for a control experiment, the experiments varied the method of cloud-wind vertical placement. These included wind insertion (1) at the level nearest the cloud-top temperature; (2) at all levels within the cloud layer as defined by the cloud-top temperature and a physical thickness; (3) at the level nearest the cloud-base; and (4) at the wind-fit level, at which the insertion wind most agrees with the guess wind.

Analyses from the four methods of level determination were compared to each other and to the control experiment. Results show that slight differences in the level of insertion can produce meaningful differences in the resulting analyses, and also confirm the value of cloud winds in data-sparse regions. Advantages and disadvantages of the wind insertion methods are discussed.

CONTENTS

1. INTRODUCTION 1

2. THE PROBLEM 3

3. THE ANALYSIS 5

   3.1 General Description 5
   3.2 Data Density Effects 6
   3.3 Area and Boundary Conditions 6
   3.4 Quality Control 9
   3.5 Effectiveness and Reliability 10

4. DATA 13

   4.1 Rawinsonde Observations (RAOBS) 13
   4.2 Cloud Motion Vectors (CMV) 13
   4.3 Synoptic Situation 16

5. PROCEDURE 19

6. LEVEL DETERMINATION METHODS 21

   6.1 Cloud-top Level 21
   6.2 Wind-fit Level 21
   6.3 Cloud-base Level 23
   6.4 Cloud Inclusive Level 24

7. RESULTS 25

   7.1 Effects of Methods on Data Distribution . . . 25
   7.2 Effects of Methods on Analysis 38

8. CONCLUSIONS 61

9. CONTINUED EXPERIMENTATION 63

ACKNOWLEDGMENTS 65

REFERENCES 67

APPENDIX A - ANALYSIS FIRST GUESS 71

1. INTRODUCTION

Historically, data assimilation has been approached largely from a dynamical aspect, with numerical modeling aspects being the primary consideration. More recently, the particular problems of real data have been addressed by work on the assimilation of orbiting satellite, vertical temperature soundings (Hayden, 1973); and on the collection of data from various sensors (Miyakoda et al., 1975). These and other studies clearly indicate that differences in characteristics among data from various types of sensors must be considered separately to ascertain how information can best be assimilated into numerical analyses.

This study is concerned with the assimilation of information from geostationary satellites, specifically, cloud motion vectors (CMV). For effective assimilation of CMV, three basic questions must be addressed: (1) Is there useful information? (2) What information (full vector wind, space gradient, vorticity only, speed only) effects the best possible assimilation? (3) What are the errors in these vectors and how can they be minimized?

Although various circumstances can produce cloud motions that are not characteristic of the wind, cloud winds have been compared with rawinsonde observations (Hubert and Whitney, 1971; Hasler, 1972; Suchman et al., 1975), with special aircraft observations (Fujita et al., 1975; Hasler et al., 1977), and with analyzed wind fields (Lemar and Bonner, 1975). These studies have shown that, in general, satisfactory winds can be derived from satellite cloud motions. Comparison of CMV with *in situ* aircraft flights have shown that CMV can have the accuracy needed for use in the sensitive divergence, vorticity, and vertical motion calculations necessary to describe the dynamics of the atmosphere (Hasler et al., 1977).

The question of determining the best information from CMV for assimilation has received much less attention. Viezee et al. (1977) found that, for two sets of SMS data and one specific analysis technique, divergence computed from the CMV was meteorologically unacceptable. The corresponding vorticity fields gave

good results. However, the analysis procedure used did not include vertical coupling, so these conclusions should be considered tentative. Further work on this question is needed.

Errors in CMV result from five major causes: navigation errors, operator errors (where man-machine methods are utilized), errors of resolution, errors due to particular clouds being unrepresentative of the wind velocity, and height computation errors. Suchman et al. (1975) have shown that the misalignment due to navigation errors is much smaller than the resolution of the original images. They also demonstrated that operator errors were minimal, and that matching an image spacial resolution with the time between images has reduced the impact of time resolution errors. Trained meteorologists interacting with the computer to compute winds, plus continuing studies such as those by Fujita et al. (1968, 1975) to pinpoint troublesome cloud features, are minimizing the errors caused by the tracking of unrepresentative clouds.

Cloud height errors, however, can be the largest source of error in the computation of CMV, as noted by Suchman et al. (1975) and other investigators. These errors occur because of incomplete knowledge of both the level at which the cloud motion is most characteristic of the wind, and of an exact method of computing the height using the limited information available. Nonetheless, for low level clouds in the tropics, retrieved winds provide an accurate representation of the wind field when the heights of the clouds are unambiguously known (Bengtsson and Morel, 1974).

2. THE PROBLEM

Current attempts to reduce cloud height errors involve improved methods of computing height at the time the cloud motion vectors (CMV) are derived. Mosher (1976a) has developed a method which corrects the measured infrared temperature for the emissivity of the cloud target, thus permitting the determination of the cloud-top temperature which is used with a standard atmosphere temperature profile to infer cloud-top height. National Environmental Satellite Service (NESS) operational procedure places all clouds which have tops below 700 mb (as defined by the IR temperatures) at the 900 mb level. This assumes that these are all low level convective clouds and that, therefore, the cloud motion is best representative of the wind at cloud base. For upper level clouds, an estimated cloud emissivity is used to adjust the measured cloud-top temperature by an empirical technique (Hubert, 1976b). Despite these complex methods, the assigned height can still be in error by as much as plus or minus 100 mb when compared to estimated "ground truth" such as rawinsonde observations, aircraft measurements or numerical results.

Since the primary utilization of CMV is in updating an objective analysis or numerical model, a redefinition of the problem is suggested. An objective analysis or numerical model's vertical structure is represented by layers at coarse resolutions. Atmospheric quantities analyzed, such as components of the wind, are assumed uniform throughout a particular level. The difficulty in determining the correct level at which to assimilate a CMV is compounded by the disparity inherent in the CMV height. Therefore, to identify the best level at which to assimilate a cloud motion vector, one must determine which analysis layer within the range of potential CMV heights is the level at which the cloud motion best represents the wind.

In addressing this problem, this study attempts to determine the effect of changes in insertion level on assimilation results, and identify the characteristics of four methods of determining the insertion level.

3. THE ANALYSIS

3.1 GENERAL DESCRIPTION

The objective analysis procedure used in this study was the National Center for Atmospheric Research (NCAR) Limited Area Multivariate Statistical Objective Analysis (Schlatter, 1975; Schlatter et al., 1976). Properties include a spherical latitude-longitude grid with a 1.25° horizontal resolution, and 10 pressure levels plus the surface in the vertical. This procedure, based on the concept of optimum interpolation (Gandin, 1963), simultaneously estimates the height and u- and v-components of the wind by applying a set of differences between a given first-guess and the observed height and wind data, to the first guess. The estimation has the form

$$\begin{bmatrix} h \\ u \\ v \end{bmatrix} = \begin{bmatrix} h_f \\ u_f \\ v_f \end{bmatrix} + \sum_{i=1}^{N} A_i \begin{bmatrix} h_i - h_{f_i} \\ u_i - u_{f_i} \\ v_i - v_{f_i} \end{bmatrix}$$

where h, u, v are the grid point values of height, u- and v-components of the wind, respectively; h_f, u_f, v_f are the first guess values of these grid point fields; h_i, u_i, v_i are observing points; h_{f_i}, u_{f_i}, v_{f_i} are first guess values at the observing points; and A_i are the difference coefficient matrices. These matrices are chosen so as to minimize the individual error variances

$$\overline{(h_t - h)^2}^s, \quad \overline{(u_t - u)^2}^s, \quad \overline{(v_t - v)^2}^s,$$

simultaneously. A subscript t indicates the true value and $\overline{(\ )}^s$ represents a seasonal average.

The height-height (h-h) correlation is modeled by a Gaussian autocorrelation curve. The remaining eight correlations involving the wind components are derived from the h-h correlation and the geostrophic approximation.

Analyses were done every six hours with persistence as the first guess. The initial first guess is a combination of a National Meteorological Center (NMC) analysis, valid at the first analysis time, and climatology (see Appendix A for details). In addition to h, u, and v, a univariate analysis of temperature was performed.

3.2 DATA DENSITY EFFECTS

Only five observations within a radius of 1500 km from the grid point are considered by the objective analysis. If only one observation is available in this range, the first guess is used without correction by observations. Thus, in a data rich region, observations in a very small area may influence the final estimate of the parameter at a grid point. In a data sparse region, however, as few as two data points, possibly far from the grid point, have influence. The weight of these distant points is necessarily much smaller, but it is readily apparent that the quality of analyses in data sparse regions cannot approach the result in data dense regions.

3.3 AREA AND BOUNDARY CONDITIONS

The area in which analyses were performed, shown in Figure 1, includes most of North America, Central America, a portion of South America, and the Eastern Pacific Ocean. This area was chosen to limit the computation time for the experiments, to include areas of good cloud motion coverage, and to include both an area of dense rawinsonde data (North America) and another area with a sparse or missing rawinsonde network (Pacific Ocean). Boundary conditions for this limited area grid are fixed; perturbations at the boundaries are reflected back into the grid. In a previous limited-area study using this analysis system, most of the grid was affected by at least one meter per second (m/s) in the wind field after five days, with the major error within five to ten degrees of the boundary (Schlatter, 1977). In order to minimize the effect of the boundary in the analysis area, the analyses in a 15° buffer at each boundary were ignored. The remaining diagnostic area is as shown in Figure 2.

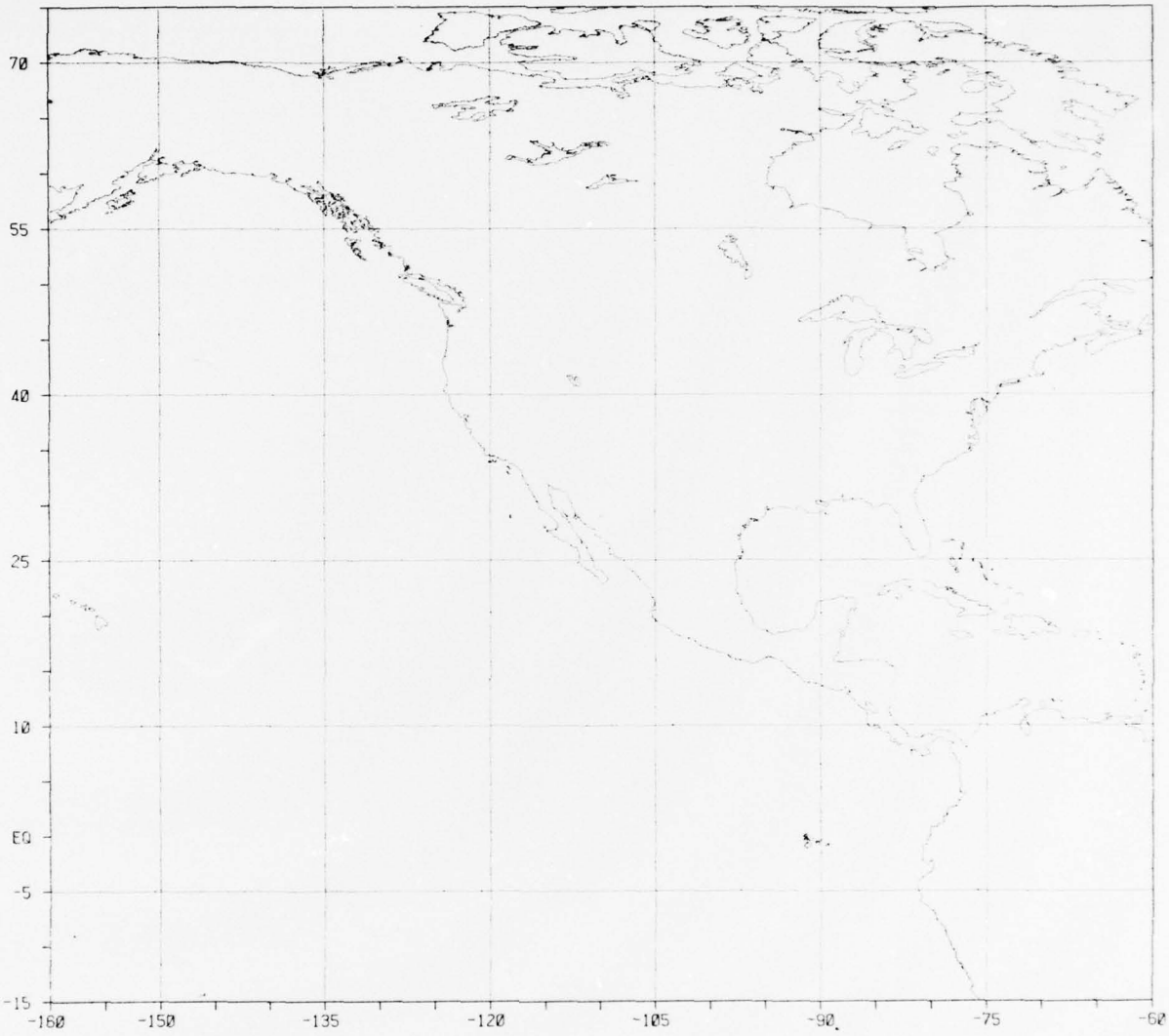

Figure 1. Geographical area in which the objective analysis was performed.

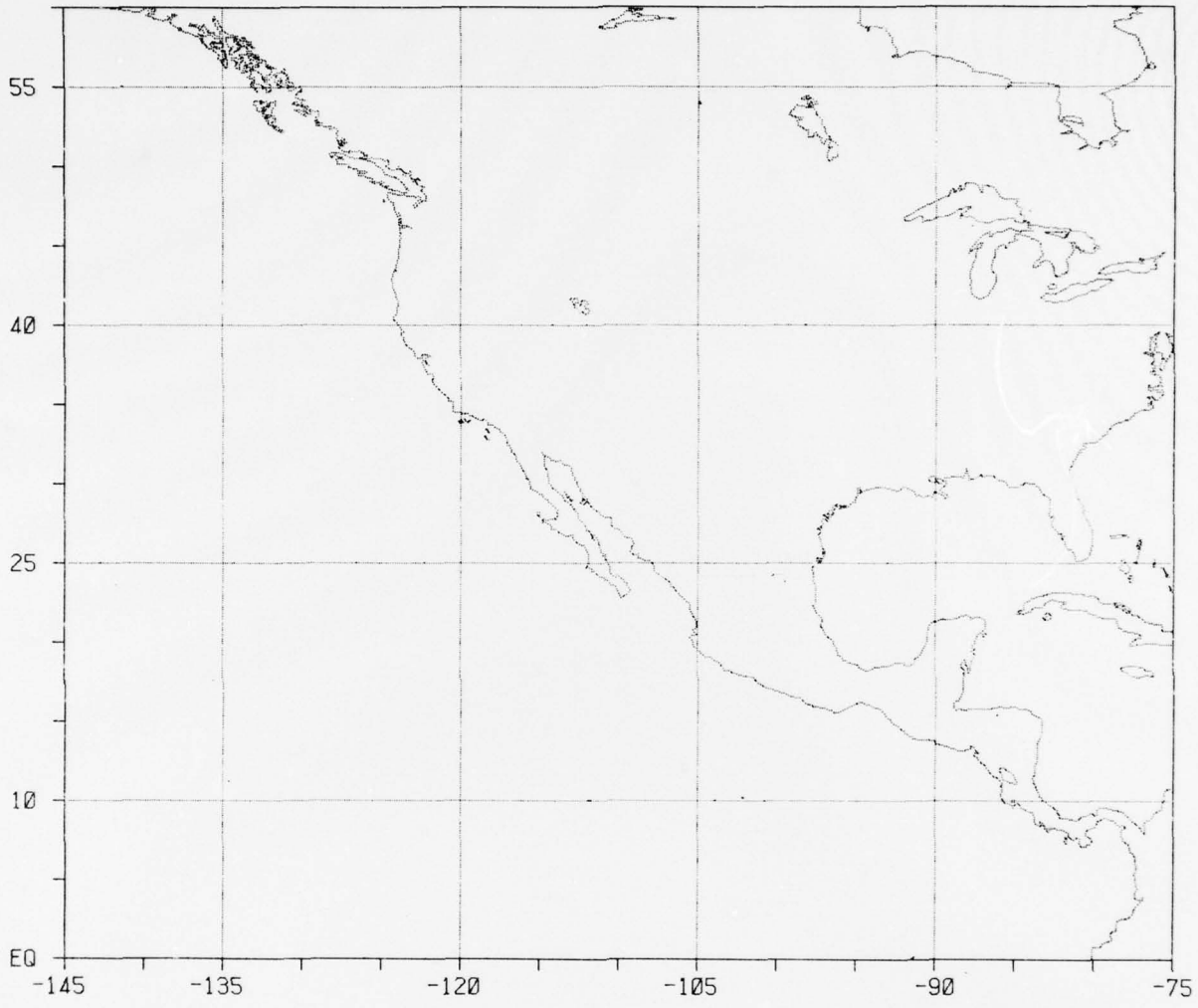

Figure 2. Geographical area in which diagnostic evaluations were performed.

3.4 QUALITY CONTROL

Three types of quality control are utilized within this analysis system.

First, an observation is discarded if it is greater than 10 times the corresponding first guess value.

Second, for each data point, the five nearest neighbors are determined, and the difference between the observation and the first guess at these points is computed. The averages of these differences of all combinations of four of the five neighbors are computed and the data point is discarded if all of these neighbors' average differences vary from the difference at the data point by more than a specified tolerance. These tolerances vary for each variable by level, as given in Table 1.

Table 1. Quality control tolerances.

Level (mb)	Height (m)	u,v (m/s)	Temperature (°C)
70	50	15	5
100	50	15	5
150	80	25	5
200	90	25	5
250	100	30	5
300	100	25	5
400	100	20	5
500	100	20	5
700	100	15	5
850	100	15	5

Third, a manual override was used for assurance of quality. Contoured plots of the resulting analysis fields were compared subjectively with a plot of the original observations on which data discarded by the automated quality control were noted. It was then possible either to discard an observation retained or to restore one rejected by the analysis, and redo the analysis procedure. This manual capability was used for only the control case in this study.

3.5 EFFECTIVENESS AND RELIABILITY

The effectiveness and reliability of this procedure, including its ability to produce analyses that conform to the data, has been demonstrated (Schlatter et al., 1976). However, particular aspects, as they relate to the current study, deserve further discussion.

In areas where the density of the data is comparable to the density of the grid points, the first guess has a minimum impact; only a very crude initial first guess causes any degradation of analysis results. However, in data-sparse regions, even after a number of time periods using a forecast as the first guess, the analysis result has been found to have little in common with the actual atmospheric state. Since persistence is used as the first guess for the current study, information cannot propagate from data-dense to data-sparse areas as it would with a forecast as first guess. In regions with no influence from the data for the entire period of the experiment, the final analysis will be identical to the initial first guess.

As noted earlier, expressions for covariances other than h-h utilize the geostrophic approximation. Figure 3 is a plot of the difference between the geostrophic wind and the analyzed wind for 500 mb at 1200 GMT on 14 December 1967. Clearly shown is the presence of a reasonable ageostrophic wind component in the resultant analysis, despite the constraint on the covariance functions.

Changes in the analysis results were anticipated when the procedure involved in the methods of determining the CMV insertion level in this study were designed. A question arose as to whether the observed changes might be due mainly to the treatment of the analysis rather than the different levels of insertion. The sensitivity of this objective analysis procedure to slight changes in the analysis configuration have also been demonstrated (Schalatter et al., 1976). This was accomplished by computing a forecast from the result of six different analysis configurations which varied the source of the first guess and the parameters analyzed. Comparisons of these forecasts show differences in root-mean-square (rms) scores of the wind and geopotential height

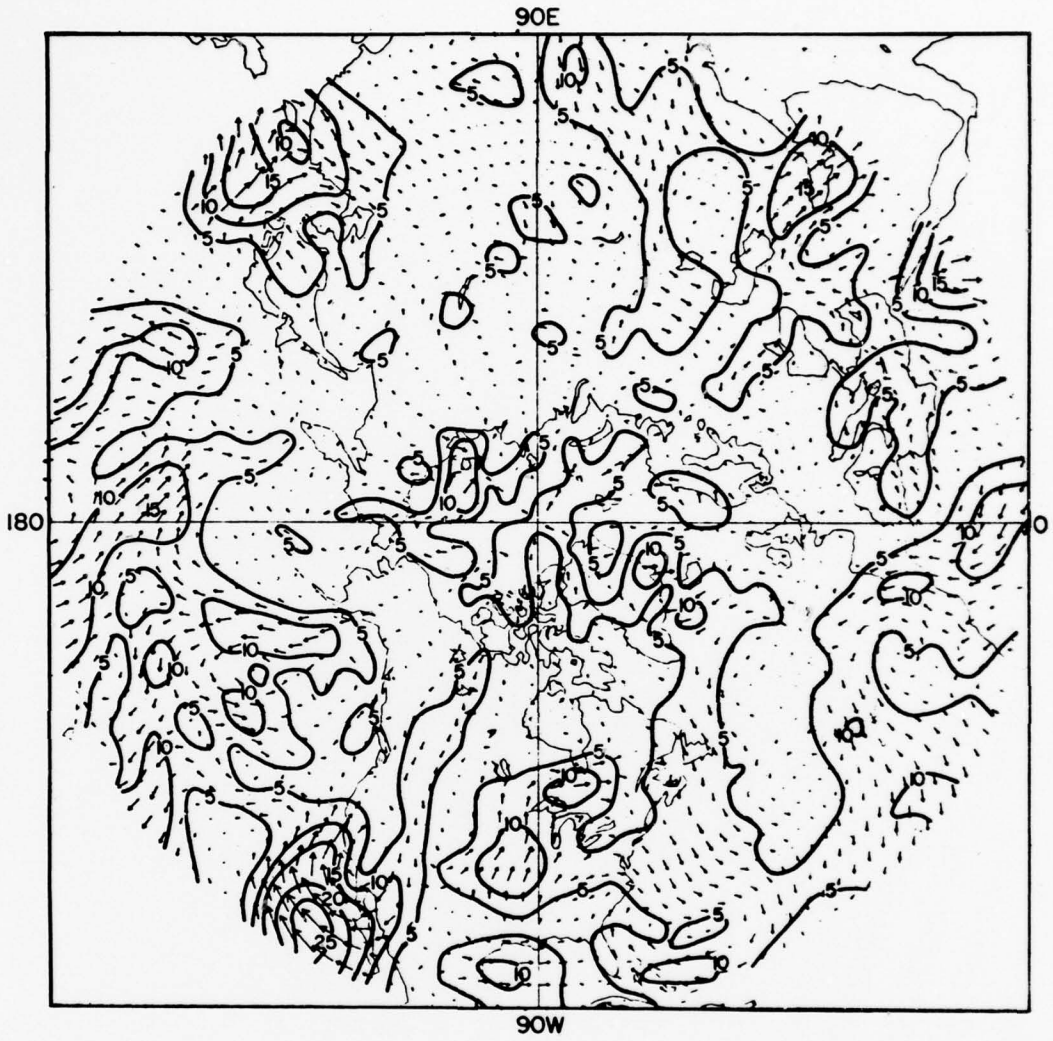

Figure 3. Presence of ageostrophic component in Northern Hemisphere analyzed wind field, obtained by subtraction of the geostrophic wind component (computed from the height field) from the analyzed wind at 500 mb for 1200 GMT, 14 December 1967. Length of vectors is proportional to the wind speed and isotachs are drawn at intervals of 5 m/sec. (After Schlatter, Branstator, and Thiel, 1976)

of only about 10 percent. This result suggests that differences in resulting analyses in the present study were due to the level differences and not to the effects of the analysis handling situations differently.

4. DATA

4.1 RAWINSONDE OBSERVATIONS (RAOBS)

RAOBS for 00 GMT, 25 January 1976, through 00 GMT, 28 January 1976, were used in all experiments. Observations at 00 GMT and 12 GMT were linearly interpolated to 06 GMT and 18 GMT to obtain RAOBS at six-hour intervals. Only those stations with reports at both 00 GMT and 12 GMT were used in the interpolation. All reports within the analysis area were used.

4.2 CLOUD MOTION VECTORS (CMV)

CMV were computed by the University of Wisconsin Space Science and Engineering Center (SSEC) on the Man-Computer Interactive Data Access System (McIDAS) during a Global Atmospheric Research Program (GARP) Data Systems Test (DST). The literature contains descriptions of the McIDAS system and its applications (Suomi, 1975; Smith, 1975; Chatters and Suomi, 1975), and the data acquisition process during the January-February 1976 DST (Mosher, 1976b; Chatters, 1976). It is important to note that these vectors were derived in real time and are not a special set derived for research purposes; therefore, the particularities of quantity and quality are those typical of an operational environment.

Two CMV were computed from three SMS-2 images (visible and infrared) at 30-minute intervals and centered at GMTs 0415, 0945, 1515 and 2245, for the period 2245 GMT, 24 January 1976, to 2245 GMT, 27 January 1976. Since the analysis was done at standard synoptic times, the averages of these two CMV were inserted at the analysis times closest to the cloud-wind center times noted above.

An example of the 850 mb data distribution for 00 GMT, 28 January (CMV center time 2245 GMT, 27 January) is shown in Figure 4. CMV are represented by wind barbs at points indicated by asterisks; an X with a wind barb and height and temperature in standard position indicates a RAOB. Units are knots, geopotential meters, and degrees celsius (kt, m, °C) respectively. The dominance of cloud motion vectors over the Pacific Ocean and of RAOBS over North America is evident. The distribution for 300 mb (Figure 5) shows

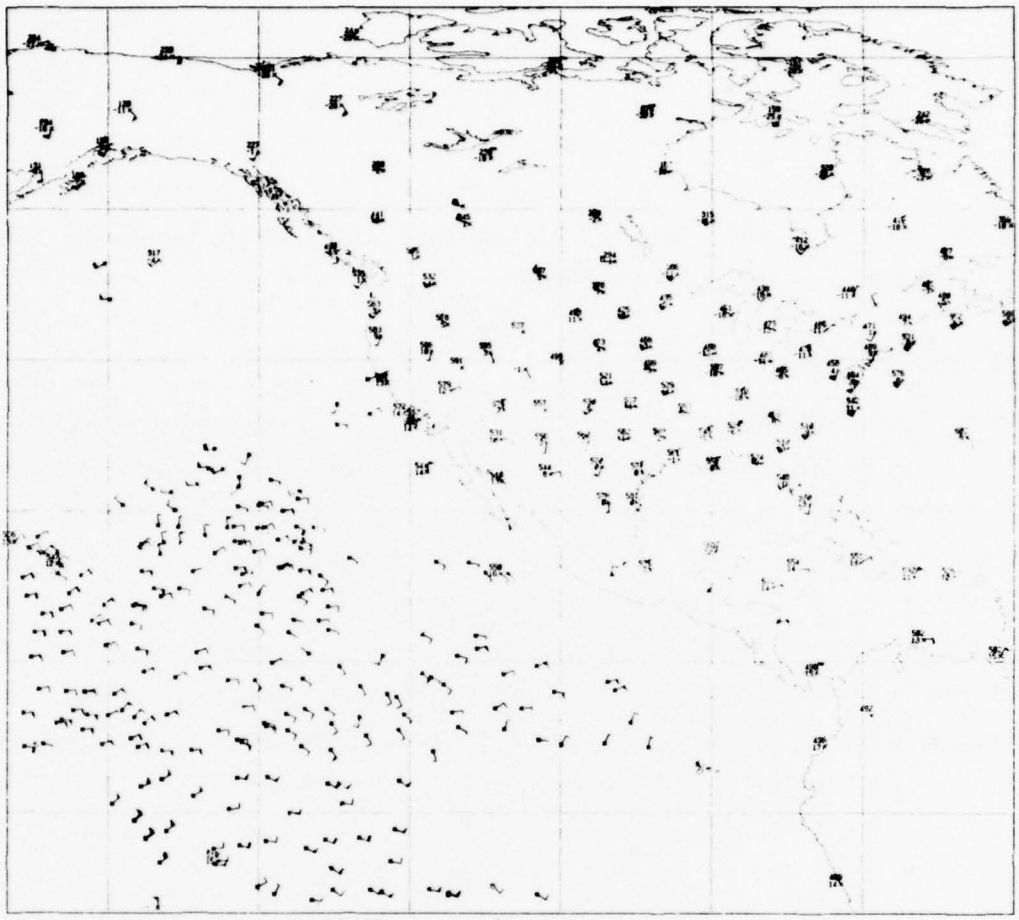

Figure 4. 850 mb data distribution, 00 GMT, 28 January 1976. Observations with numeric designations for height and temperature are rawinsonde reports. Observations with wind designation only are CMV tracked at times between 2215 and 2315 GMT. Units are knots, geopotential meters and degrees centigrade.

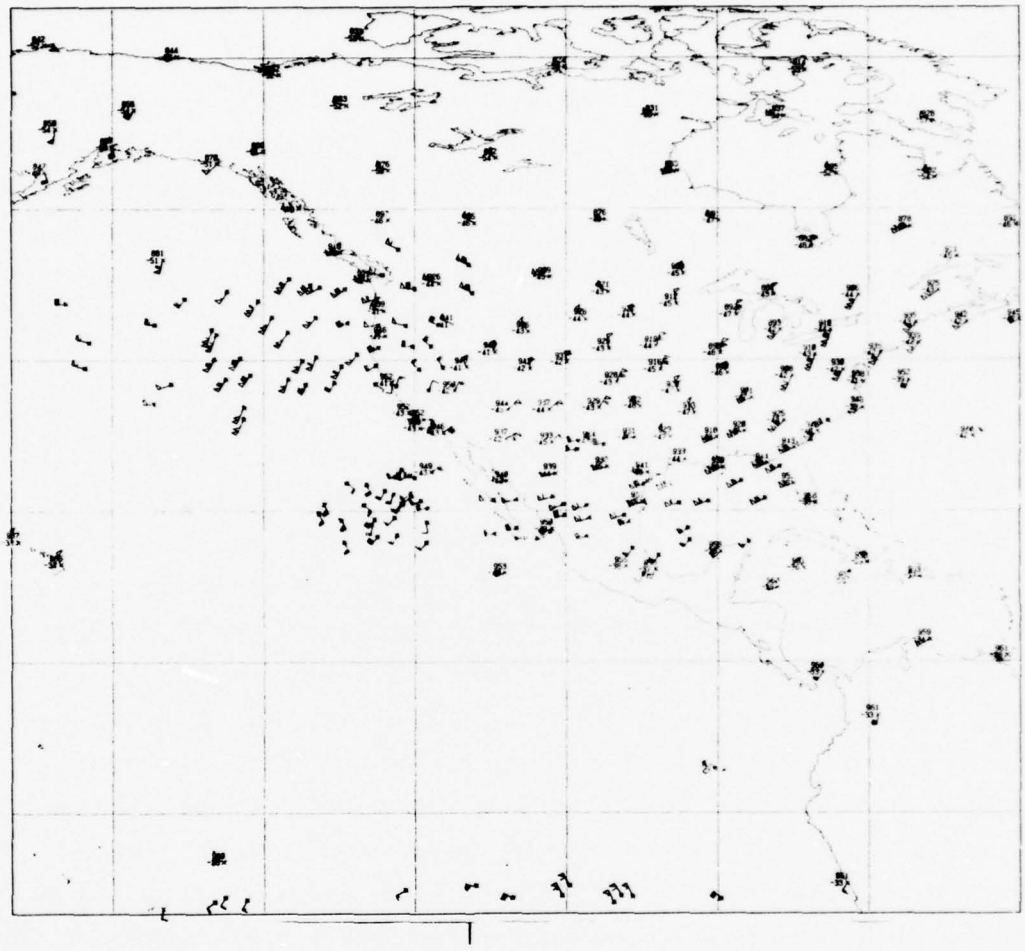

Figure 5. Same as Figure 4, but for 300 mb.

two areas of CMV : one extends across Mexico and the Gulf of Mexico area, and the other across the northwest United States and adjacent Pacific Ocean. Although the level determination methods utilized in this study altered the specific vertical location of the cloud motion vectors, these figures illustrate the general distribution of the data used.

In addition to wind information, the McIDAS also computed cloud-top temperature, cloud thickness, and approximate height (in hundreds of millibars). The cloud-top temperature was determined from the infrared data and an emissivity which, in turn, was derived from the optical thickness. Details of the computation of optical thickness and physical thickness have been described by Mosher (1974).

One important characteristic of the method by which the cloud-top temperature and thickness are determined merits special mention. Standard procedure for the McIDAS operator during this DST was to visually identify a "fleet" of clouds, (i.e., a group of clouds related geographically, considered to be at the same level, and possessing similar characteristics (GARP, 1978)), and then to compute the cloud-top temperature and thickness for a few cloud elements and assign the subjective average of these values to all vectors computed within this fleet. This was done to increase the speed of the tracking procedure and to utilize the operator's experience to minimize level assignment errors. In this study, however, individually determined cloud-top temperature and thickness would have been of value since each vector's level is determined individually in comparison with a first guess field.

4.3 SYNOPTIC SITUATION

The Fleet Numerical Weather Central (FNWC) operational analysis of geopotential height at 850 mb for 00 GMT on 25 and 28 January (Figure 6) shows the synoptic situation for the period. A blocking high dominated the situation off the west coast of the United States; it moved only slightly eastward and expanded to encompass the Rocky Mountains during the period of this study. A

00GMT 25 JAN

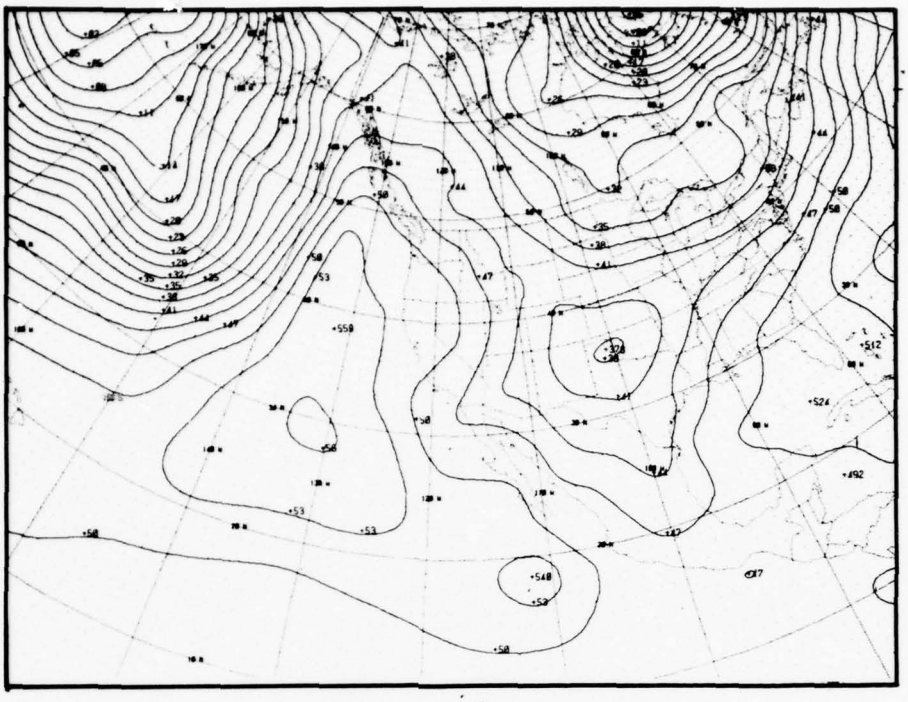

00GMT 28 JAN

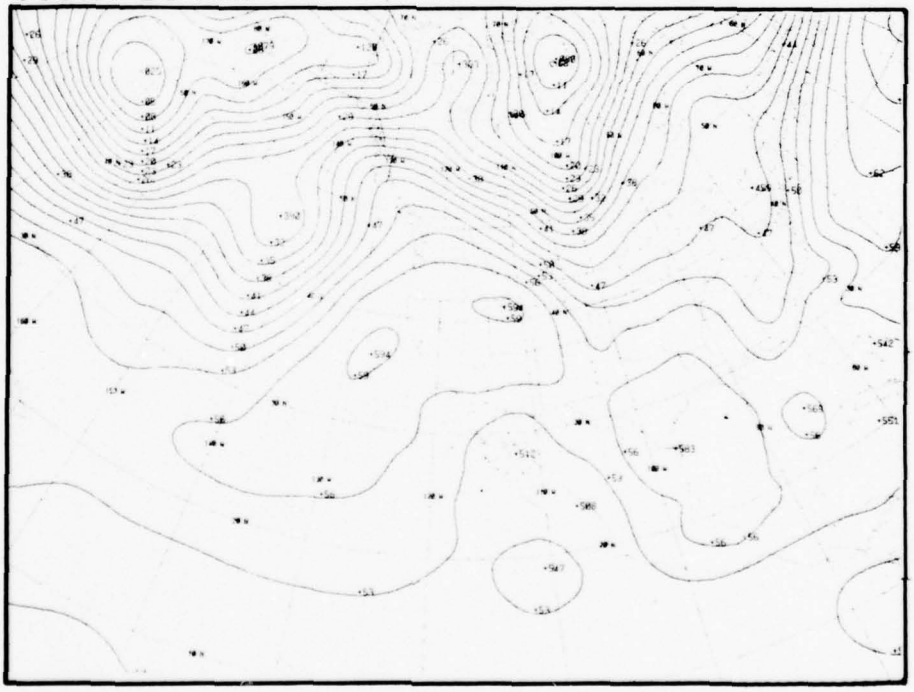

Figure 6. Synoptic situation depicted by the Fleet Numerical Weather Central 850 mb height analysis for 00 GMT, 25 January 1976 (top) and 00 GMT, 28 January 1976 (bottom) plotted on a polar stereographic grid with a 30 m contour interval.

low in northeast Canada gave rise to thunderstorms down the eastern seaboard of the United States on 25 January, but moved quickly out of the region. A new trough was centered over the central states at the beginning of the period; this storm weakened and moved into the eastern part of the country on 28 January as another trough moved into the midwest from central Canada.

In the tropics on 25 January (not shown in Figure 6), there was a large area of cloud activity between latitude 20°N and a well-defined intertropical convergence zone (ITCZ) at 5°N, and longitude 145°W to 115°W. The structure of clouds in the region slowly lost its form during the analysis period and became more sparse in nature; the strongest portion was in the eastern part of the region, off the coast of Mexico, by 28 January.

5. PROCEDURE

A control experiment and four other assimilation experiments were conducted using the procedures shown schematically in Figure 7. In the control case, which included only the RAOB data, an analysis was performed every six hours using analysis fields from the previous synoptic time as the first guess and inserting RAOB data. For the cases in which RAOBS and CMV were inserted, an analysis was also performed every six hours using the previous analysis as the first guess. The RAOB data were subjected to an error elimination: all RAOBS discarded by the quality control procedures in the control case for the same time were eliminated from the data set before assimilation by the analysis in subsequent cases. CMV pressure heights computed by McIDAS (as explained in Section 4) were replaced by a pressure level determined by one of four methods, each of which used the previous analysis as the basis for the determination. At the initial time, the resultant analysis from the control case for 00 GMT, 25 January was used.

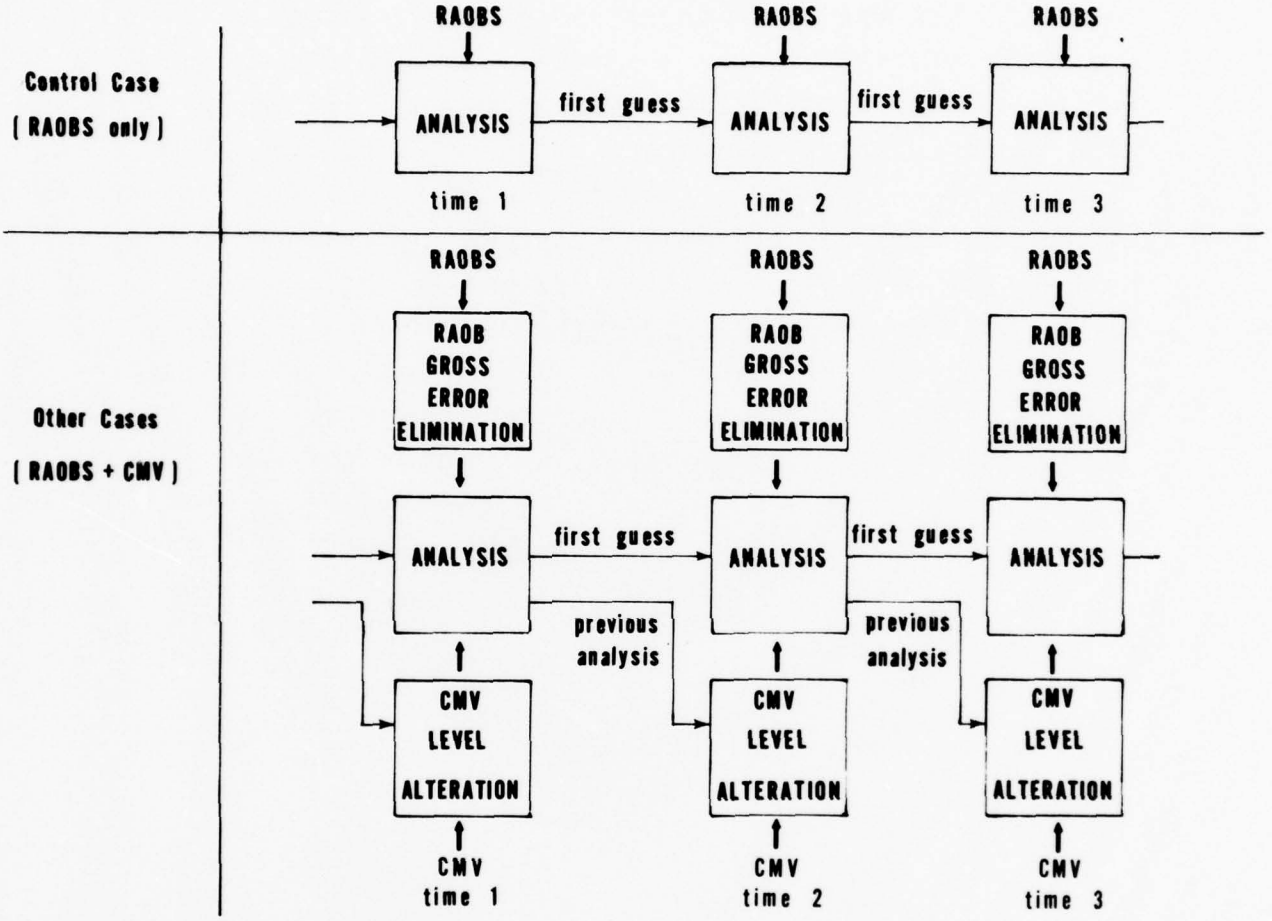

Figure 7. Assimilation procedures for the rawinsonde-observation-only case and the rawinsonde-plus-CMV cases. Vertical arrows show data flow between various steps of the procedure. Horizontal arrows indicate use of the first guess and previous analysis results by the current analysis cycle.

6. LEVEL DETERMINATION METHODS

Four methods for defining the assimilation level were tested. In each method, the given pressure height computed by McIDAS was replaced by one of the 10 analysis pressure levels. The vectors themselves were not altered; only the level at which these values were assimilated was changed.

To illustrate these methods, Figure 8 shows a cloud spanning three objective analysis levels for which a CMV has been computed. The following descriptions assume that this is the average state of the cloud over the hour period during which the motion occurred.

6.1 CLOUD-TOP LEVEL

The McIDAS wind tracking system determines a pressure height of the top of the cloud being tracked, based on the cloud-top temperature (corrected IR temperature) in relation to a standard atmospheric temperature profile. Since the CMV is to be inserted in an objective analysis, a better estimate of the correct analysis level for assimilation can be obtained by using the analysis itself rather than a standard atmosphere. In this method, CMV were assimilated at the level at which the cloud-top temperature best corresponded to the analyzed temperature as obtained from the previous analysis, at the grid point nearest the CMV observation.

6.2 WIND-FIT LEVEL

So-called level of best fit (LBF) techniques have been used in the past to investigate the accuracy of cloud winds in relation to rawinsonde observations (Hubert and Whitney, 1971; Davis et al., 1973). CMV were assigned heights which minimized the vector difference between the cloud motion and the wind profile of a nearby rawinsonde. Davis et al. (1973) found that the LBF for convectively-based clouds was lower than the cloud-top height derived from infrared measurements, and that the LBF for thin cirrus clouds was higher.

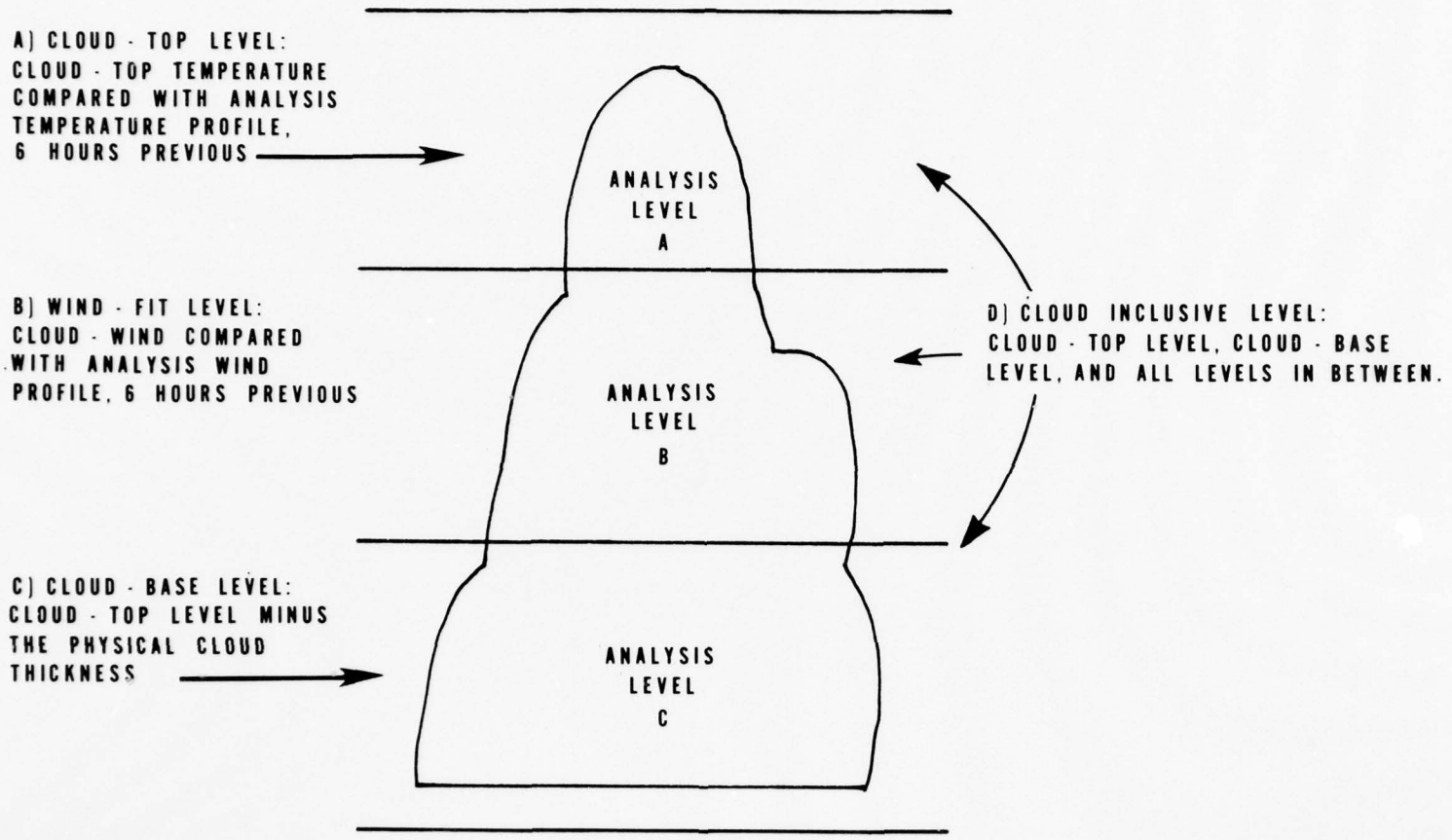

Figure 8. Four methods for determining the analysis insertion level. For a cloud spanning three analysis levels, the Cloud-top level method (A) assigned the top level; the Cloud-base level method (C) assigned the lower level; and the Cloud Inclusive level method (D) assigned all three levels as the correct insertion level. The Wind-fit level method (B) selected any one of the three.

A similar technique, but one designed to minimize the ambiguity attributed to LBF techniques, was used for the second method. The vector difference between the cloud motion vector and the analysis wind profile at the nearest grid point for the previous time was minimized to determine the "wind-fit level."

Davis (1976) cites a problem in using the LBF which also affects the wind-fit level determination method used here: the recurrence of similar winds at different levels. This is particularly serious since cloud motions may resemble an analysis wind at more than one level, especially for upper level cloud motions, and so allow the assignment of a level at a much different height from the actual cloud. The wind-fit minimization in this study was confined to only those analysis levels plus or minus two levels from the level in which the original McIDAS height assignment fell. Although this restriction still allows the discrepancies to occur, inspection revealed no obvious examples of this.

6.3 CLOUD-BASE LEVEL

Hasler et al. (1977) and Hasler and Shenk (1977) have measured cloud motion and wind at various levels simultaneously from aircraft in a number of samples of clouds. Their experiments have shown that oceanic trade wind and subtropical high regime cumulus clouds move within 1.3 m/s of the wind at cloud base, within the error limits of the experiments. Isolated cirrus clouds were found to move within 1.6 m/s of the cloud layer mean wind. The mean wind for cirrus may likely fall within the same analysis level as the cloud top, but the cloud-base wind for cumulus will in many cases fall within a different level from that of the cloud top.

Thus, in the third method, the CMV was assigned to the cloud-base level. The cloud-top level was determined, as in the first method, from the cloud-top temperature and the temperature profile for the previous analysis at the nearest grid point. The physical cloud thickness obtained during cloud tracking (as described in Para. 4.2) was then subtracted from the height at this cloud-top level. The analysis level within which this reduced height occurred was assigned to the CMV as its assimilation level.

6.4 CLOUD INCLUSIVE LEVEL

As noted by Bengtsson (1975), the motion of a cloud is affected by shear and mixing processes; therefore, a CMV should be interpreted as an integrated effect of horizontal and vertical motions. Recent studies (Smith and Hasler, 1976; Hubert, 1976a) have suggested that cloud motions near disturbances in the tropics do not represent the wind at one particular level. In light of these results, the Cloud Inclusive method was devised.

This method assigned the vector value to every level which encompassed the cloud being tracked (i.e., every level in between and including cloud-top and cloud-base levels). The cloud-top level and cloud-base level were determined by the methods described in Paras. 6.1 and 6.3 above, respectively. The CMV was assimilated at both of these levels and any intervening levels. Cloud top and cloud base for many CMV fell in the same analysis level, and the vector was inserted at only one level; for most other clouds the thickness was not great enough to include more than two levels.

Although not physically realistic, this technique allowed each level which might have received the CMV information, depending on the method of level determination, to be affected by the information.

7. RESULTS

Two different aspects of each of the level determination methods were examined: (1) Effects of the methods on the vertical and temporal distribution of the CMV, and (2) effects on the resultant analysis after the vectors were assimilated. A third aspect, that of producing a forecast with the analysis results, was outside the scope of this study.

7.1 EFFECTS OF METHODS ON DATA DISTRIBUTION

If the first guess is a reasonable estimate of the state of the atmosphere for the analysis time, then the data inserted should be in relative agreement with this first guess, but adjust it toward a more accurate solution. A comparison between the data and the first guess has value in evaluating the information content of the data. Mean RMS differences, $\bar{D}_k$, by level between the CMV after level determination and persistence were computed for each method. These differences are shown in Figure 9. $\bar{D}_k$ was given by:

$$\bar{D}_k = \frac{1}{M}\sum_{j=1}^{M}\sqrt{\frac{1}{N_{j,k}}\sum_{i=1}^{N_{j,k}}(U_{p_{i,j,k}} - U_{s_{i,j,k}})^2 + \frac{1}{N_{j,k}}\sum_{i=1}^{N}(V_{p_{i,j,k}} - V_{s_{i,j,k}})^2}$$

where $N_{j,k}$ is the number of SMS observations at level k and time j, and M is the number of analysis times. U_p and V_p are the u- and v-components of the persistence first guess at the nearest grid point, and at level k and time j. Similarly, U_s and V_s are the components of the cloud-wind at level k and time j. Above 200 mb, the number of total observations entering into the computation was quite small, making the results less significant.

Also plotted, in addition to the three methods for determining the assimilation level that were utilized for the full period of this study, were the mean RMS differences between the cloud winds at the McIDAS computed levels and the Control case's persistence first guess. The Cloud Inclusive case is not shown because it was utilized for only one day of data. Since the goal of these methods' utilization was an improvement in the analysis, the RMS differences

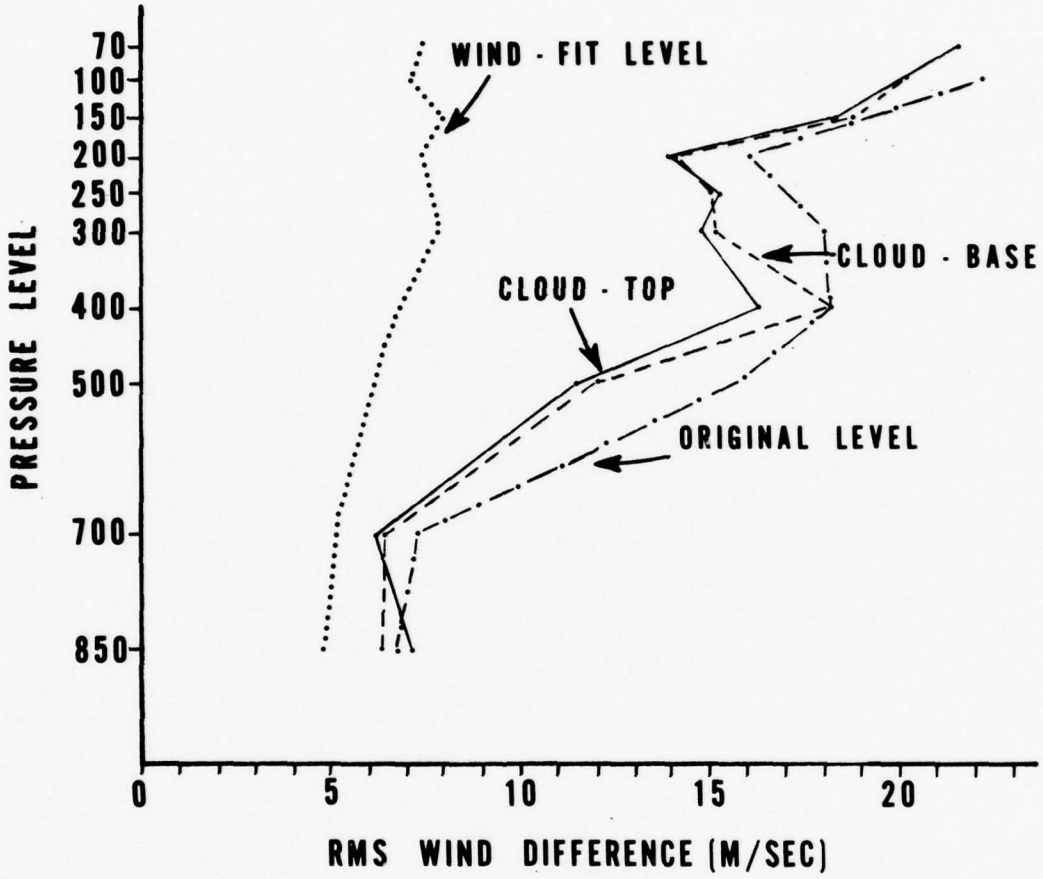

Figure 9. Temporal mean root-mean-square differences between the persistence wind vectors and the CMV after determining the insertion level for the Wind-fit, Cloud-top and Cloud-base methods. RMS differences between Control persistence and the original levels are also shown.

should be less than or equal to those for the data at original levels. As Figure 9 shows, this was true for all methods at all levels except for the Cloud-top case at 850 mb. The Wind-fit result was by far in the closest agreement with the first guess, but should have been by definition. It represents the best attainable result with the given data if the cloud wind values retain their identity (and persistence is used as first guess).

Because only the height was changed for each CMV, the number of vectors at a particular time was the same for each experiment, except for the Cloud Inclusive method. (In this method, vectors for thick clouds may have been assigned to more than one level.) However, due to the different methods of determining the level, the number of vectors at each level varied among experiments. Temporal distributions of the respective methods for a particular analysis level were investigated by plotting the number of observations at one time as a percent of the vertically totaled observations for that time. This was done for the lower levels (Figure 10) and the near-tropopause levels (Figure 11).

Fundamental differences between methods are immediately apparent upon inspection of Figure 10. Generally, a larger percentage of vectors in the Cloud-top case were placed at 700 mb than at 850 mb, while the reverse was true for the Cloud-base case (although not to as great a degree). This is to be expected in light of the algorithms utilized to determine the analysis level. In the Cloud-top case at 06 GMT, 26 January, the percentages were atypical due to a large decrease in the total number of lower level vectors at that time, particularly at 700 mb.

The 700 mb graph for the Cloud Inclusive case was similar to the Cloud-top case; the 850 mb trace resembled the Cloud-base case. Only one day of the three-day period was completed for the Cloud Inclusive experiment because it appeared to be a middle state between the Cloud-top and Cloud-base methods. This was especially true of the upper-level vectors, as shown in Figure 11.

The Wind-fit distributions demonstrated a tendency to equalize the number of CMV on the vertical. The 850 mb level showed a

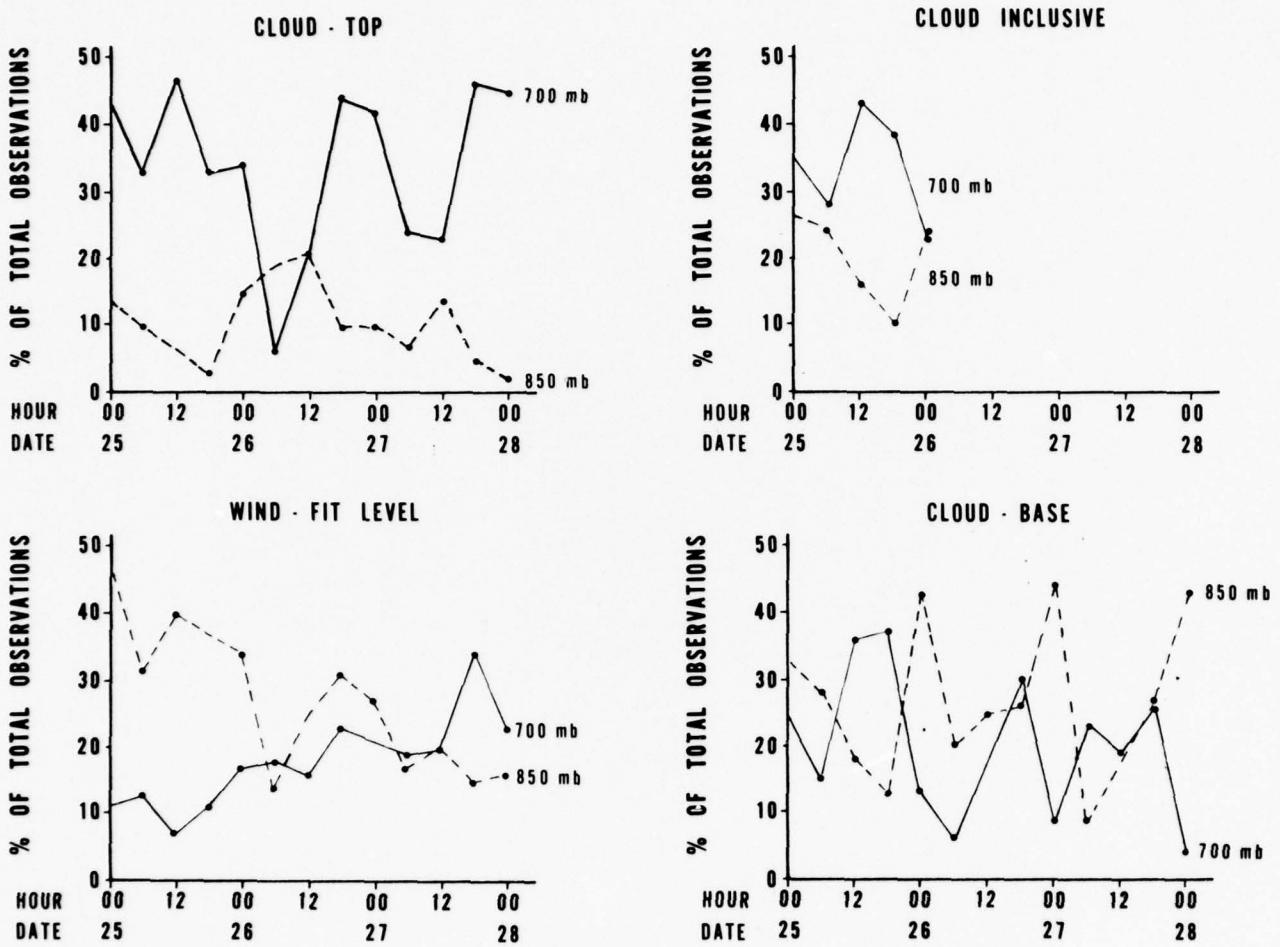

Figure 10. Temporal variation of the number of CMV observations at one time plotted as a percent of the vertically totaled observations for that time. 700 mb and 850 mb levels are shown for all four methods.

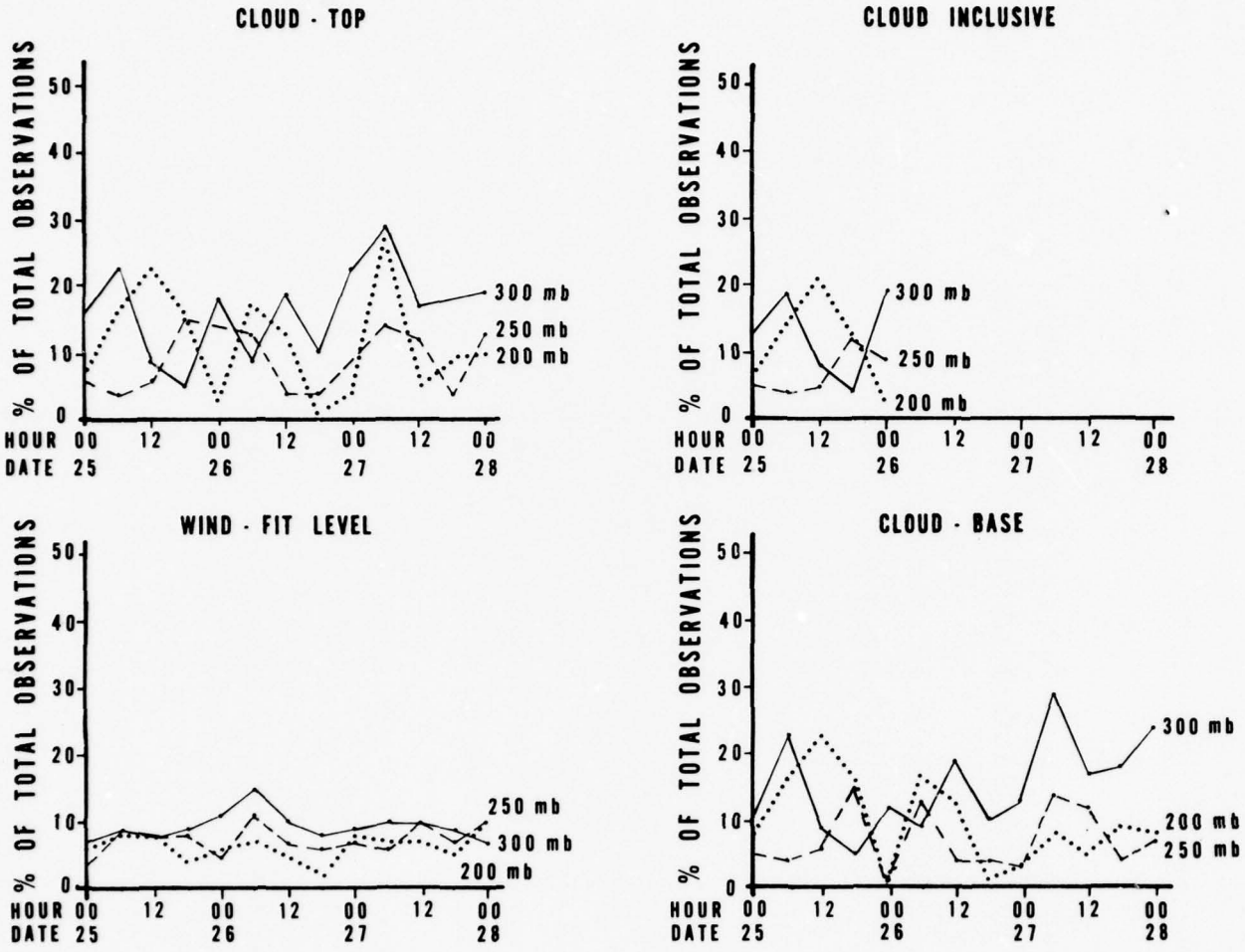

Figure 11. Same as Figure 10, but for 200, 250, and 300 mb levels.

decrease from a large percentage at the beginning of assimilation to a mid-range percentage at the end. The 700 mb percentages, however, increased from low to mid-range values. To see if this trend continued, the level assignment program was run for 06 GMT on 28 January using 00 GMT SMS satellite data (06 GMT data was not available); results gave values of 17% at 850 mb and 22% at 700 mb. An increasing number of winds assigned to 850 mb at the initial time were assigned to 700 mb as time progressed, until the number of observations at the two levels was essentially equal. This peculiar tendency encouraged closer examination of the effects of the Wind-fit method.

Additional disturbing characteristics presented themselves when the relationship between the level assigned by the various methods and the original McIDAS-assigned level was examined. Table 2 shows the number of vectors at each original level for 00 GMT, 28 January, which was assigned to each new level by the level determination methods. After assignment, the Cloud-top and Cloud-base distributions at the tropopause levels contained vectors which was originally at or near these levels. For the Wind-fit method, however, vectors originally at 300 mb were relocated to as many as seven different levels ranging from 700 to 150 mb. Since CMV have a height error (usually within 100 mb), the Cloud-top and Cloud-base cases' vertical distributions seem reasonable, while the distribution for the Wind-fit case does not.

Plots in Figure 12 illustrate the number of CMV at each level as a percentage of the total CMV at all levels for one time. Dashed lines show the range of these percentages over the three-day period; the solid line is the mean over the period. Where insertion was at the cloud top, a large peak occurs at 700 mb with smaller peaks at 200 and 300 mb. The Cloud-base method is similar, but the lower level maximum is at 850 mb. The Wind-fit method produces a smooth curve, increasing downward, with a smaller variance in the values over the period. The Cloud-base result is the most realistic with respect to studies showing cloud-wind quantity maximum near 300 and 900 mb (Hasler and Shenk, 1977; Hubert and Whitney, 1971).

Table 2. Vertical reassignment for 00Z 28 Jan.

(a) Cloud-Top Method

Level Before (mb)	Level After (mb) 850	700	500	400	300	250	200	150	100	70	Totals
900	8	208	0	0	0	0	0	0	0	0	216
800	2	18	0	0	0	0	0	0	0	0	20
700	0	0	6	0	0	0	0	0	0	0	6
600	0	0	0	0	0	0	0	0	0	0	0
500	0	0	0	0	0	0	0	0	0	0	0
400	0	0	0	0	9	2	0	0	0	0	11
300	0	0	0	12	85	39	0	2	0	0	138
200	0	0	0	0	0	23	37	0	0	0	60
100	0	0	0	0	0	0	15	13	6	21	55
Totals	10	226	6	12	94	64	52	15	6	21	506

(b) Cloud-Base Method

Level Before (mb)	Level After (mb) 850	700	500	400	300	250	200	150	100	70	Totals
900	216	0	0	0	0	0	0	0	0	0	216
800	2	18	0	0	0	0	0	0	0	0	20
700	0	3	3	0	0	0	0	0	0	0	6
600	0	0	0	0	0	0	0	0	0	0	0
500	0	0	0	0	0	0	0	0	0	0	0
400	0	0	0	11	0	0	0	0	0	0	11
300	0	0	0	12	95	29	0	2	0	0	138
200	0	0	0	6	27	4	23	0	0	0	60
100	0	0	0	0	0	0	15	13	6	21	55
Totals	218	21	3	29	122	33	38	15	6	21	506

(c) Wind-Fit Method

Level Before (mb)	Level After (mb) 850	700	500	400	300	250	200	150	100	70	Totals
900	73	95	48	0	0	0	0	0	0	0	216
800	5	3	12	0	0	0	0	0	0	0	20
700	3	3	0	0	0	0	0	0	0	0	6
600	0	0	0	0	0	0	0	0	0	0	0
500	0	0	0	0	0	0	0	0	0	0	0
400	2	1	2	1	2	0	3	0	0	0	11
300	0	12	13	28	23	20	22	20	0	0	138
200	0	0	0	7	10	17	8	4	6	8	60
100	0	0	0	0	0	12	20	8	9	6	55
Totals	83	114	75	36	35	49	53	32	15	14	506

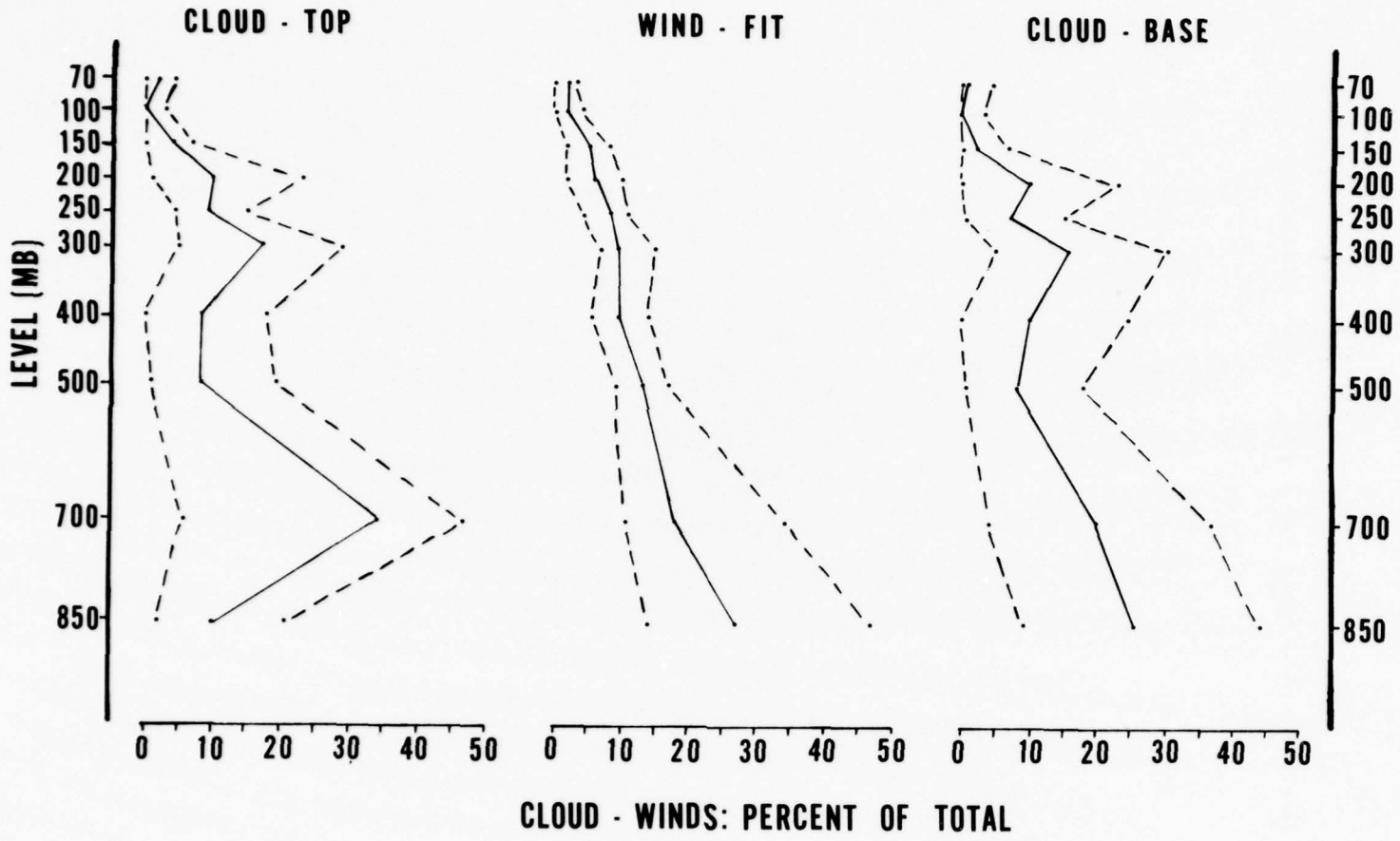

Figure 12. Number of CMV at each level, plotted as a percentage of the total vectors at all levels for a particular time. Dashed lines indicate the range of values over the three-day period; the solid lines show the mean percentages over the period.

The vertical distribution for a small area of the Pacific Ocean was determined for the 2245 GMT, 27 January, data. The distribution is depicted in Figure 13 for the three methods and for the original McIDAS vectors. The area boundaries are 32° to 10° north latitude and 145° to 126° west longitude. Individual motion vectors are denoted by numerals indicating the levels at which the particular method assigned them. From this, the distribution in the vertical can be discerned by grouping the observations by fleets. Note that the original level assignment was to the nearest 100 mb, so there were no 850, 250, or 150 mb vectors for this illustration; 800 mb vectors were plotted at 850 mb. The visible and IR images for the same area and time are shown for comparison in Figure 14.

The similarities in fleet boundaries between the distribution generated by the Cloud-top and Cloud-base methods are readily evident. They agree in general with those of the original level assignments. The major difference is that the Cloud-top method assigns levels a level higher than the Cloud-base case, particularly at low levels. Both distributions agree well with the original images. Note that the Cloud-base algorithm assigns the upper portion of the distribution to 300 mb and the southeast portion to 250 mb. This two-level formation also appears in the images.

Although the basic distribution is the same for the Wind-fit case, the vectors have been assigned to a greater variety of levels. The fleet concept becomes difficult to apply. Vectors are also assigned to unreasonable levels compared to the satellite images, such as the 70, 100, and 150 mb vectors in the northwest quadrant of the storm. Of course, this method's unreasonable assignment in comparison with the images does not preclude it from giving a useful analysis. The best level for assimilation of a vector may not be the most realistic level, just the one most representative of the wind.

One other point deserves mention. Vectors which were at the same level for all three methods were identified, and their distribution in the vertical and in time are shown in Table 3. The

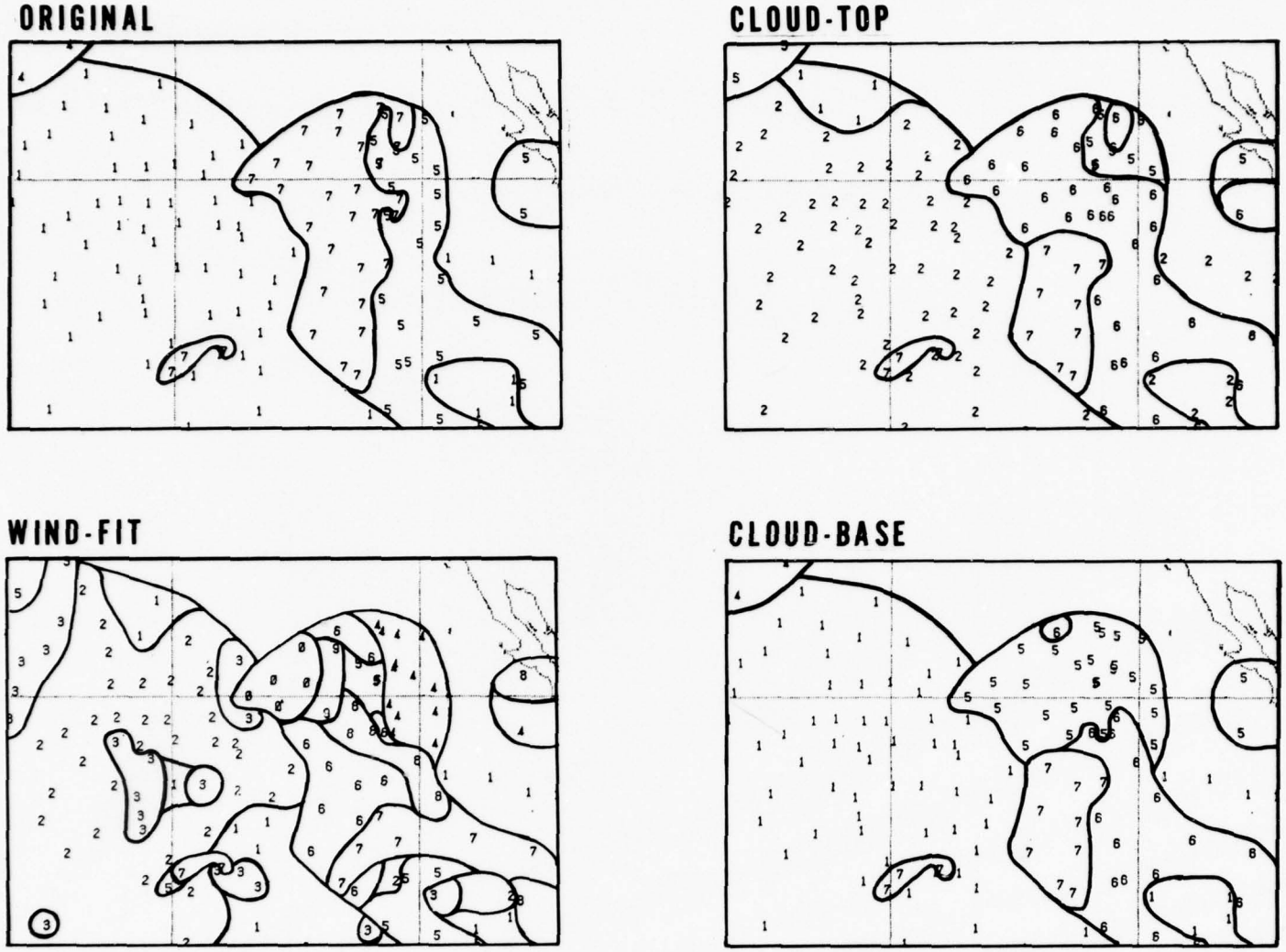

Figure 13. Spatial data distribution over an area of the Pacific Ocean with boundaries 32°N to 10°S and 145°W to 126°W for three cases and the original McIDAS levels, at 00 GMT, 28 January 1976. Each number represents one CMV and refers to its insertion level as follows: 1=850 mb, 2=700 mb, 3=500 mb, 4=400 mb, 5=300 mb, 6=250 mb, 7=200 mb, 8=150 mb, 9=100 mb, and 0=70 mb.

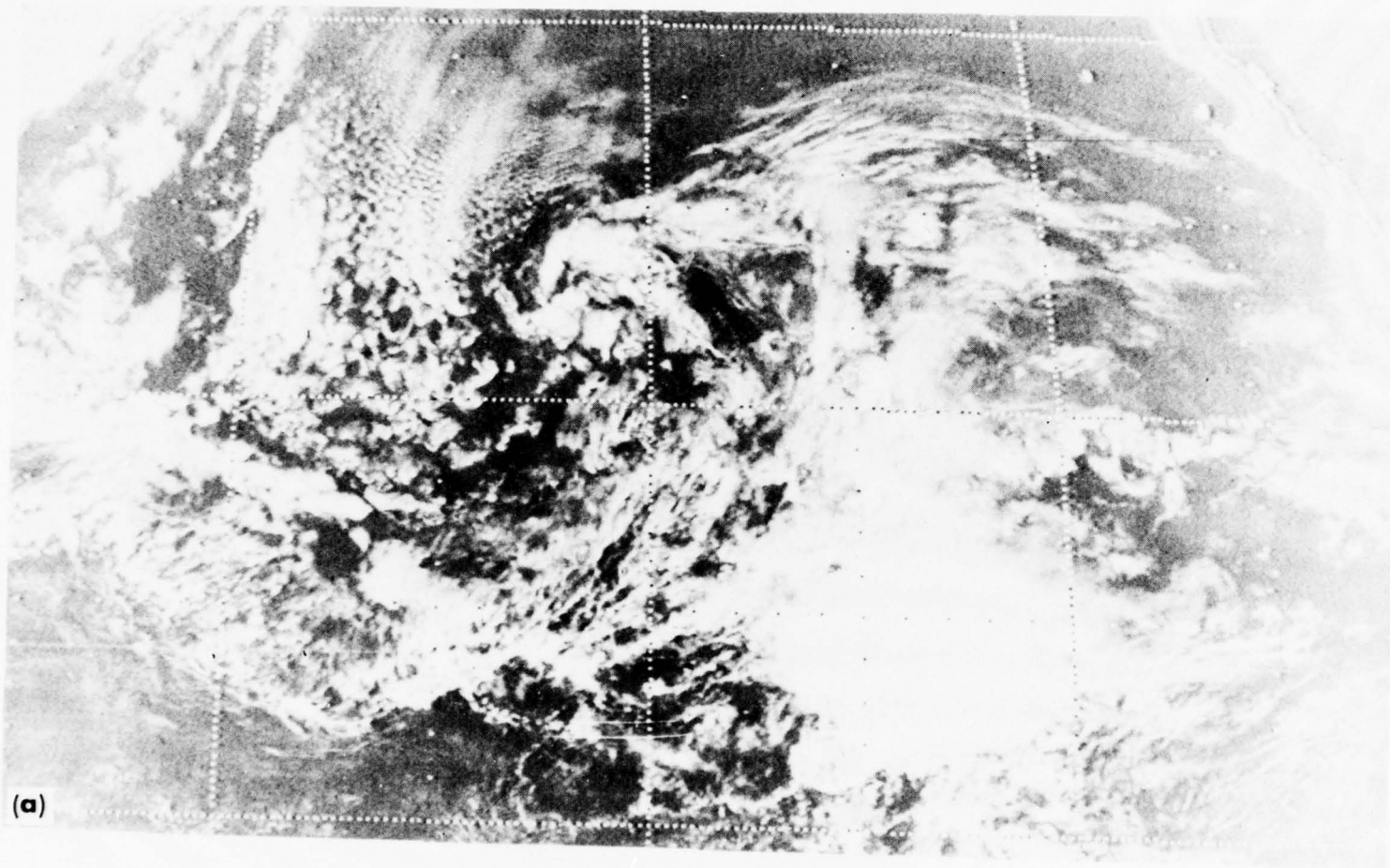

Figure 14. (a) Visible and (b) infrared SMS-2 images for the same area and time as shown in Figure 13.

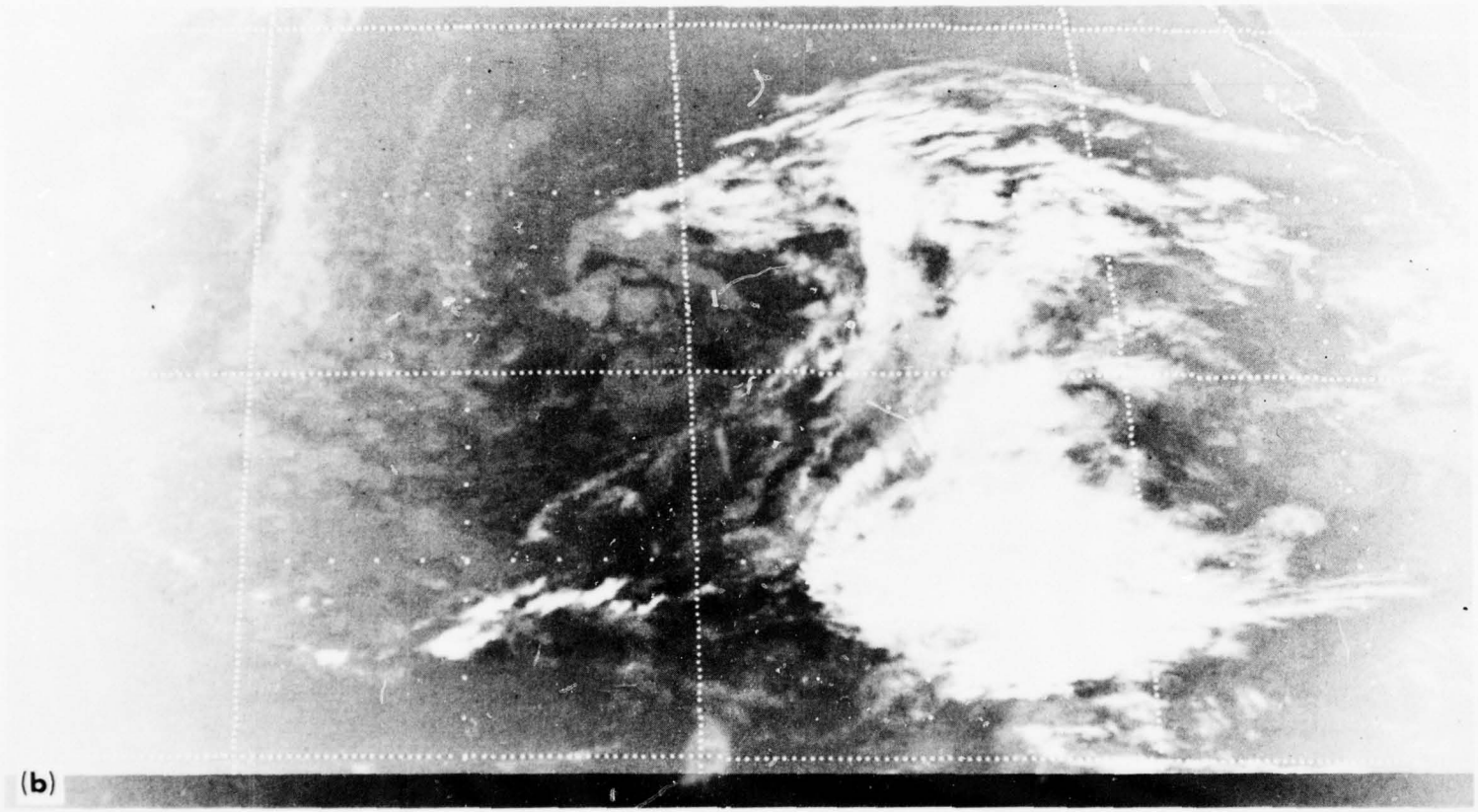

Figure 14. Continued.

Table 3. Number of vectors common to all methods at each level.

Level (mb)	25 Jan 00Z	06Z	12Z	18Z	26 Jan 00Z	06Z	12Z	18Z	27 Jan 00Z	06Z	12Z	18Z	28 Jan 00Z	
70	0	0	0	0	0	0	5	0	0	1	0	0	2	
100	0	0	1	0	0	0	0	0	0	0	0	0	0	
150	0	0	0	0	0	2	0	0	3	4	0	1	3	
200	0	0	0	9	0	7	8	0	3	4	0	4	15	
250	0	0	3	10	1	9	2	2	3	7	0	2	3	
300	4	2	2	7	9	3	10	6	12	32	7	7	12	
400	6	5	0	6	3	9	3	20	2	0	0	4	2	
500	2	0	0	2	3	12	16	8	1	16	0	1	0	
700	0	0	0	10	4	8	17	35	24	37	0	49	2	
850	50	31	22	7	45	33	46	16	45	15	38	5	2	
Total	62	38	27	51	65	83	107	87	93	116	45	73	41	
% of total possible	11	10	6	11	10	23	26	21	10	22	7	22	8	AVG=14

values for the percentage of total possible vectors for each time ranged from 6% to 26% with a mean of 14%. The fact that only a small percentage of vectors were placed at the same level by all three methods is an indication of the difference in the level assignment results of the methods. Approximately 85% of the vectors at each time for a particular method are at different levels than in the other experiments.

7.2 EFFECTS OF METHODS ON ANALYSIS

Streamline analyses at the 850 mb level for 00 GMT, 25 January, one cycle after the beginning of the analysis, are shown in Figure 15 for the Control and Cloud-base cases. These show essentially the analysis without and with cloud motion vectors, respectively. Over the U.S. and Canada, regions covered satisfactorily with rawinsonde data, the analyses are nearly identical. But in areas of the Pacific Ocean such as south of Baja near the southern grid boundary (area outlined) where few rawinsonde are available, the cloud winds force a southeasterly flow on what is a northwesterly flow when no CMV are used. Film loops of the original SMS images encompassing this time confirm the southeasterly analysis.

Figure 16 shows the same streamline analysis as Figure 15, only for the Cloud-top, Cloud Inclusive and Wind-fit experiments. Cloud-top, Cloud-base, and Cloud-Inclusive cases are nearly identical; isotach and height analyses and all parameters at other levels showed this same similarity after just one cycle. The Wind-fit case result also is very similar to the others, but does show differences such as the cyclonic flow off the coast of South America and less pronounced perturbations in the equatorial mid-Pacific region.

To show the vertical difference between level determination methods after the first cycle, meridional cross-sections of wind fields were constructed for each method as shown in Figure 17. Shown are the u-component wind plots at 130° west longitude for Control, Wind-fit, Cloud-top, Cloud-Inclusive, and Cloud-base methods. The entire analysis field was used for convenience, but

values for the percentage of total possible vectors for each time ranged from 6% to 26% with a mean of 14%. The fact that only a small percentage of vectors were placed at the same level by all three methods is an indication of the difference in the level assignment results of the methods. Approximately 85% of the vectors at each time for a particular method are at different levels than in the other experiments.

7.2 EFFECTS OF METHODS ON ANALYSIS

Streamline analyses at the 850 mb level for 00 GMT, 25 January, one cycle after the beginning of the analysis, are shown in Figure 15 for the Control and Cloud-base cases. These show essentially the analysis without and with cloud motion vectors, respectively. Over the U.S. and Canada, regions covered satisfactorily with rawinsonde data, the analyses are nearly identical. But in areas of the Pacific Ocean such as south of Baja near the southern grid boundary (area outlined) where few rawinsonde are available, the cloud winds force a southeasterly flow on what is a northwesterly flow when no CMV are used. Film loops of the original SMS images encompassing this time confirm the southeasterly analysis.

Figure 16 shows the same streamline analysis as Figure 15, only for the Cloud-top, Cloud Inclusive and Wind-fit experiments. Cloud-top, Cloud-base, and Cloud-Inclusive cases are nearly identical; isotach and height analyses and all parameters at other levels showed this same similarity after just one cycle. The Wind-fit case result also is very similar to the others, but does show differences such as the cyclonic flow off the coast of South America and less pronounced perturbations in the equatorial mid-Pacific region.

To show the vertical difference between level determination methods after the first cycle, meridional cross-sections of wind fields were constructed for each method as shown in Figure 17. Shown are the u-component wind plots at 130° west longitude for Control, Wind-fit, Cloud-top, Cloud-Inclusive, and Cloud-base methods. The entire analysis field was used for convenience, but

a. CONTROL

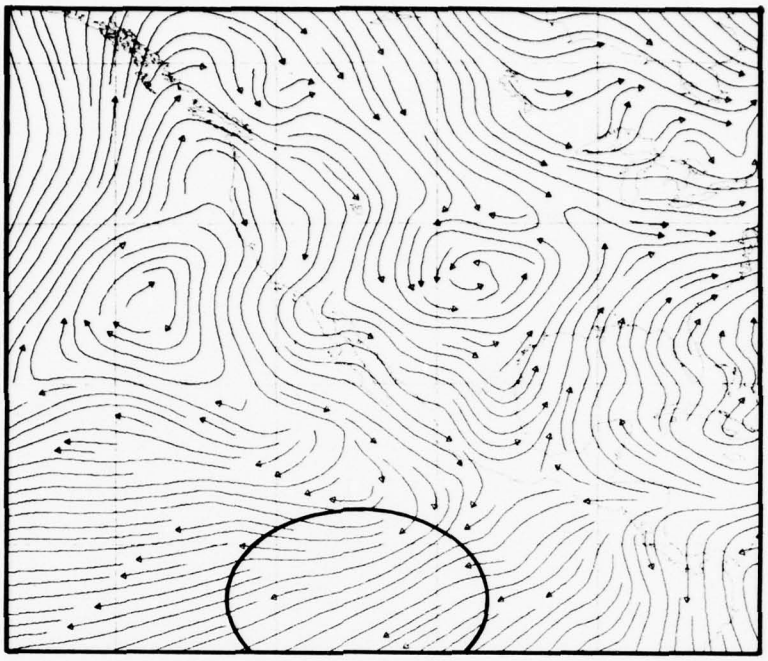

b. CLOUD-BASE

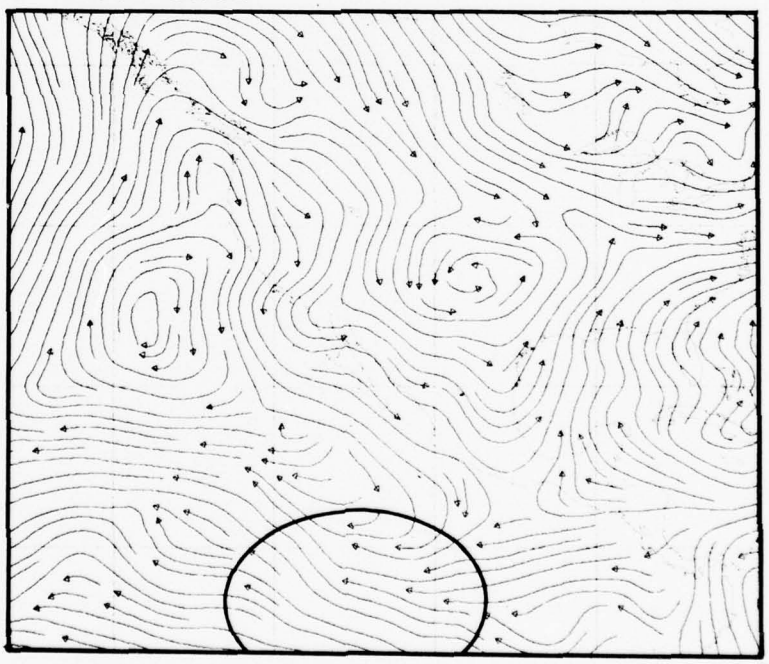

Figure 15. 850 mb streamline analyses, 00 GMT, 25 January 1976, for (a) Control and (b) Cloud-base cases.

a. CLOUD-TOP

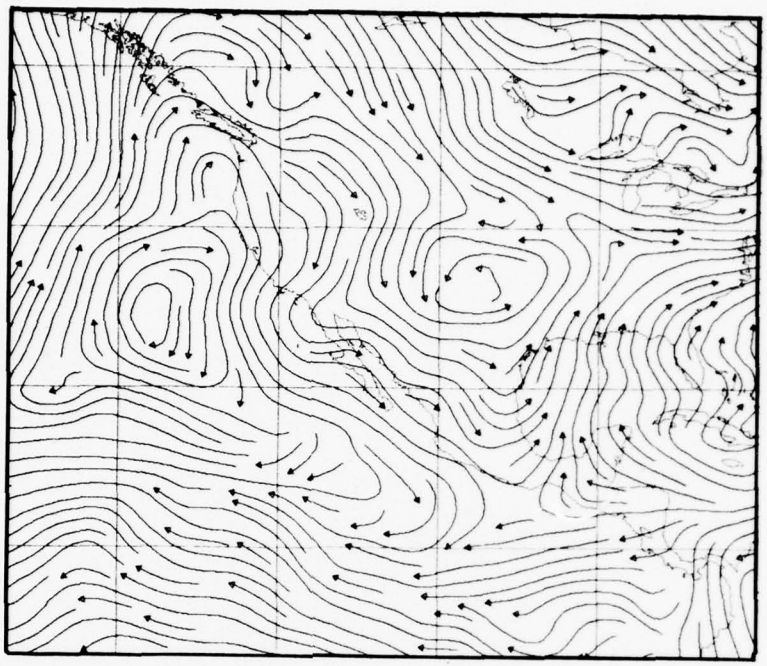

b. CLOUD INCLUSIVE

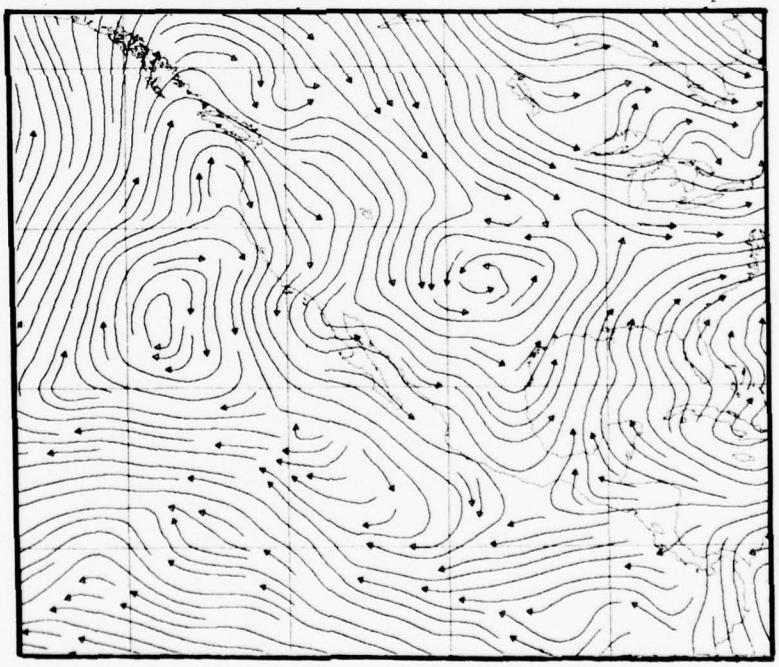

Figure 16. Same as Figure 15, but for (a) Cloud-top, (b) Cloud Inclusive, and (c) Wind-fit cases.

c. WIND-FIT

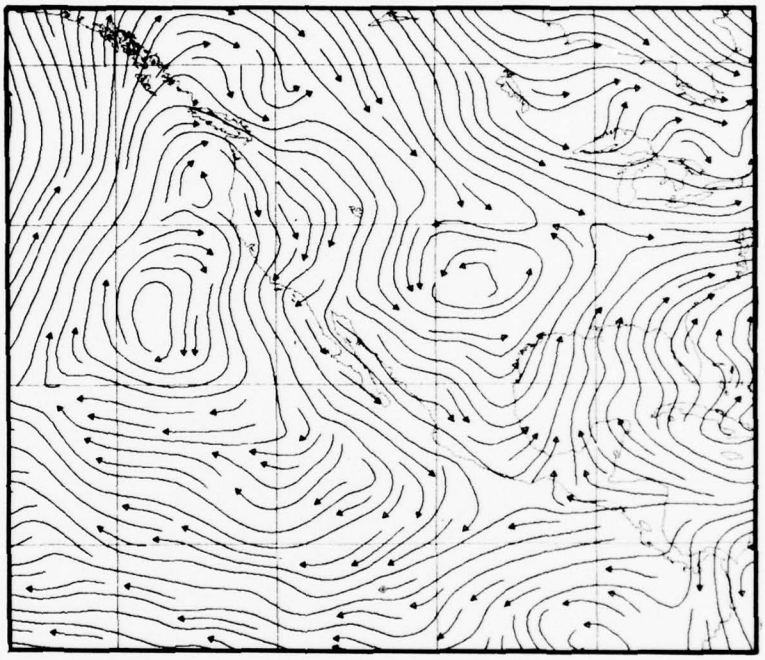

Figure 16. Continued.

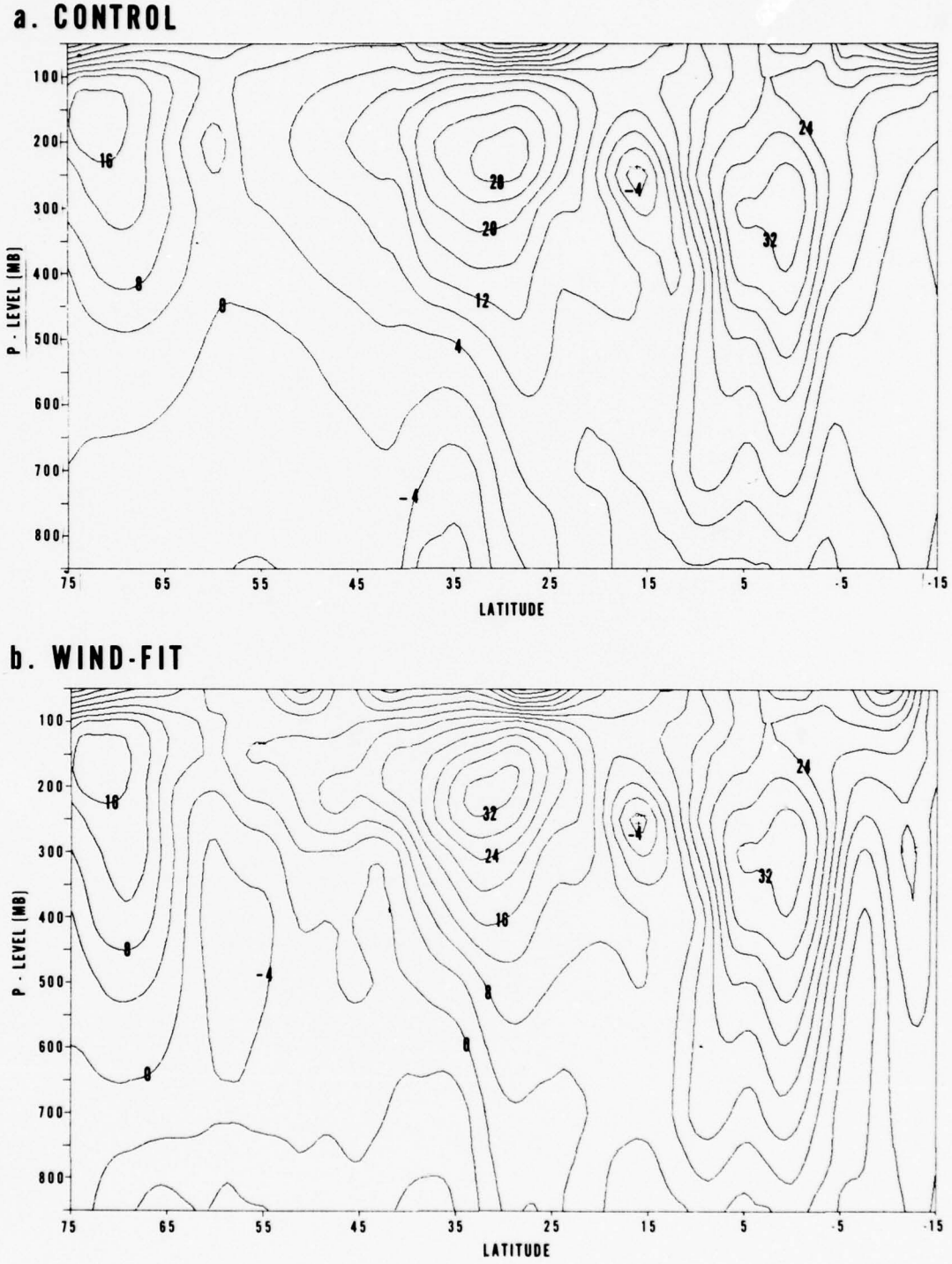

Figure 17. Meridional cross sections for the u-component of the wind at 130°W longitude for (a) Control, (b) Wind-fit, (c) Cloud-top, (d) Cloud Inclusive, and (e) Cloud-base cases, 00 GMT, 25 January 1976. Contour interval is 4 m/sec.

c. CLOUD-TOP

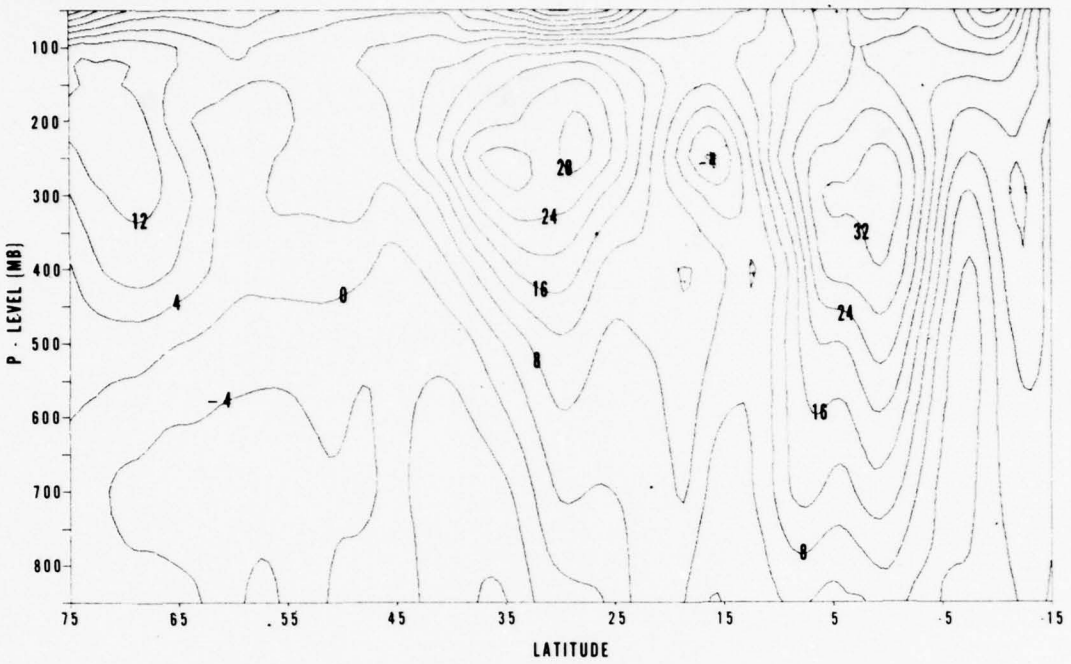

d. CLOUD INCLUSIVE

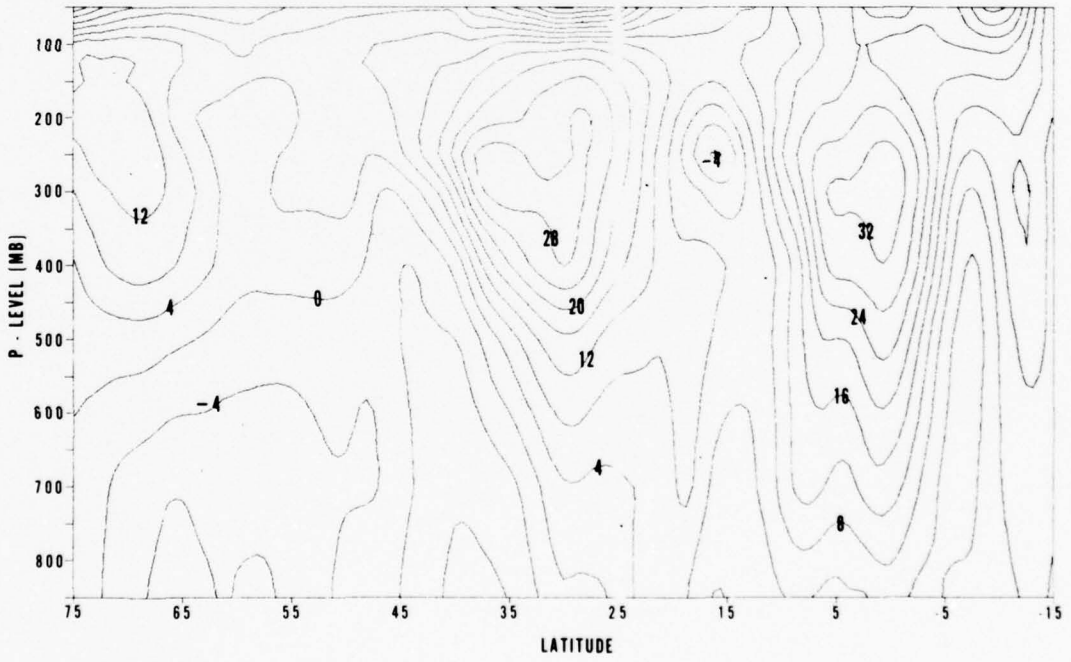

Figure 17. Continued.

e. CLOUD-BASE

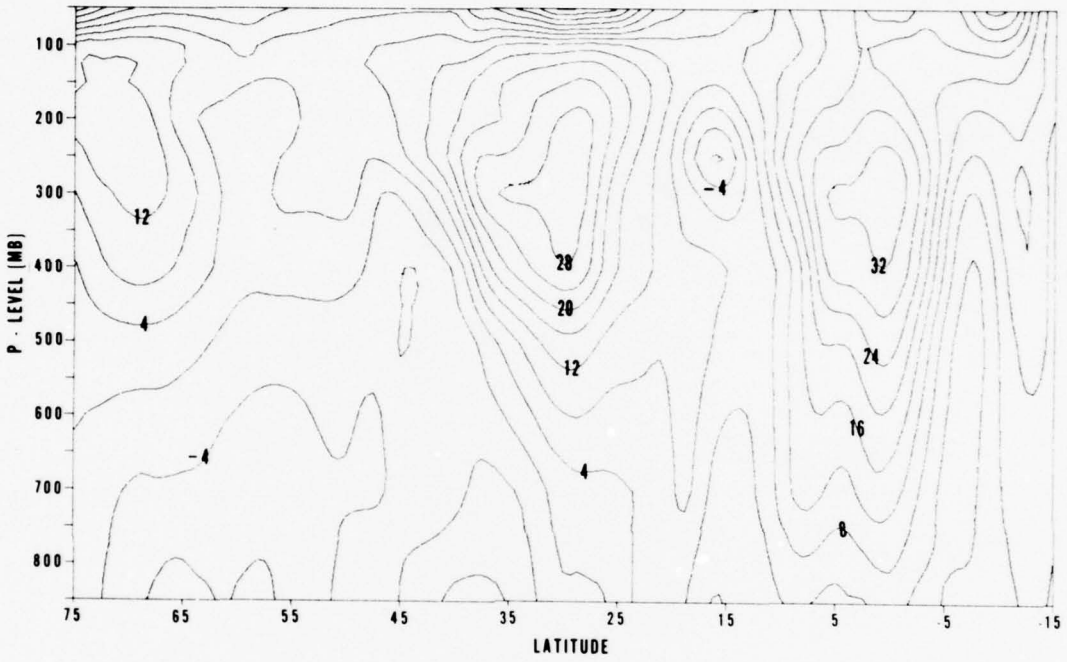

Figure 17. Continued.

after only one cycle boundary effects should not be pronounced. The vertical coordinate is pressure level.

There is relative agreement between all cases; differences exist in strength and position of the upper-level mid-latitude jet and in low-level easterly flow north of 40°N. The Control and Wind-fit cases are largely the same except for a strenthening of both of these flows. The three IR temperature-based cases are nearly identical except that the Cloud-top case double jet maximum is at 27°N and 34°N and 250 mb; the Cloud-Inclusive triple maximum is at 27°N, 30°N and 34°N, and between 200-300 mb; and the Cloud-base case double maximum is located at 30°N and 34°N and 300 mb. Notice that the Cloud-top case locates the jet higher than the Cloud-base case, and that the Cloud-Inclusive case is a combination of base and top methods. Similar results were evident in the v-component cross-section (not shown). A set of cross-sections through 90°W, a rawinsonde-rich area in the middle of the U.S., gave results which were nearly identical to each other.

Thus, after the first analysis cycle, a comparison of results from the various methods showed few differences. The only evident variations were in the location, strength, and structure of the jet maximum.

Since each execution of the analysis uses persistence as a first guess, each assimilation of the three-day period multiplies the effect of each method of level determination. To illustrate that the use of persistence does not lead to an unreasonable analysis after three days, height analyses were compared for 00 GMT on 28 January. Figure 18 shows the Fleet Numerical Weather Central (FNWC) operational analysis and the Cloud-top method result at the 850 mb level for approximately the same area. The FNWC analysis used a polar stereographic grid. General features are the same; small perturbations in the Cloud-top analysis are a result of persistence. Despite the fact that no forecast was used in the cycle, generally good analyses resulted even after three days.

FNWC ANALYSIS

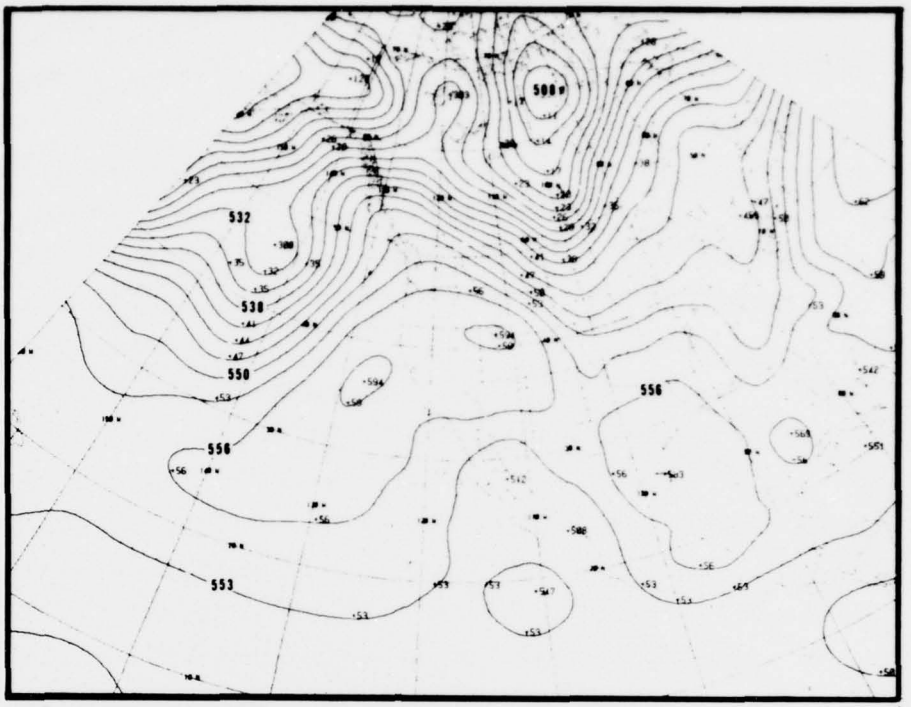

CLOUD-TOP ANALYSIS

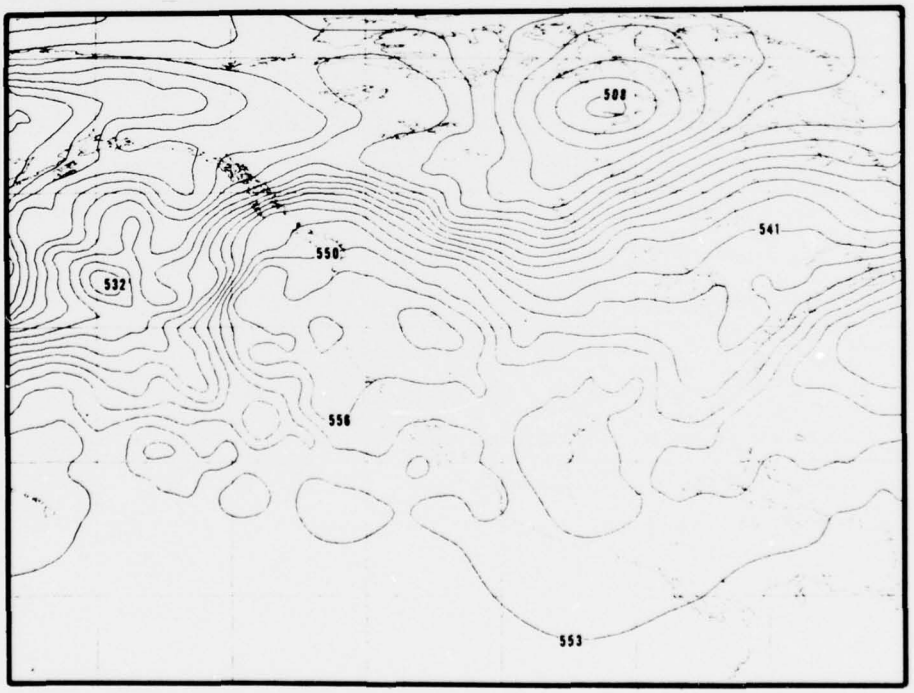

Figure 18. Comparison of the Fleet Numerical Weather Central 850 mb geopotential height analysis with Cloud-top method analysis field for 00 GMT, 28 January 1976. Contour interval is 30 m/sec. FNWC field is polar stereographic grid; Cloud-top analysis is latitude-longitude grid.

Since a large number of CMV were inserted at the 300 mb level in all of the experiments, the 300 mb streamline analyses were selected to indicate the effects of three days of assimilation on the experiments. Isotach, height, and streamline analyses had the same general characteristic for most levels. Figure 19 shows these streamlines for 00 GMT, 28 January, for the Control case and for each level determination method: Wind-fit, Cloud-top and Cloud-base. The Cloud-Inclusive case was not run past one day due to its similarity to the Cloud-top and Cloud-base cases.

Differences between the methods are subtle but definitive. There are two anticyclonic patterns evident in the equatorial region of the Wind-fit case which do not appear in the Control case or other methods. This feature began to appear a day earlier in the assimilation, and continued to develop, so it is not solely an effect of the data for the last time period. Such a flow is not suggested by satellite images at the same time; it appears to be a result of the Wind-fit case's characteristic of placing opposing cloud winds (which should be at very different levels) at the same level.

All three level determination methods introduce a perturbation into the Pacific flow west of the Baja Peninsula. This motion appears to be realistic as seen in the satellite images (Figure 14), and is more evident in film loops. The cyclonic structure developed by the Cloud-base case is particularly representative. Again, rawinsonde-dense regions are nearly identical.

Comparison of these analyses is difficult. To achieve a better grasp of the differences between methods, the RMS differences of the wind components between each method and the Control case were plotted. Figure 20 shows these differences for the 250 mb level. The small differences over the United States' dense rawinsonde network are readily evident. CMV have little effect over this area regardless of which method is used. The larger differences in middle Canada are the effects of CMV at 12 GMT and 18 GMT of 26 January in an area of few RAOBS.

a. CONTROL

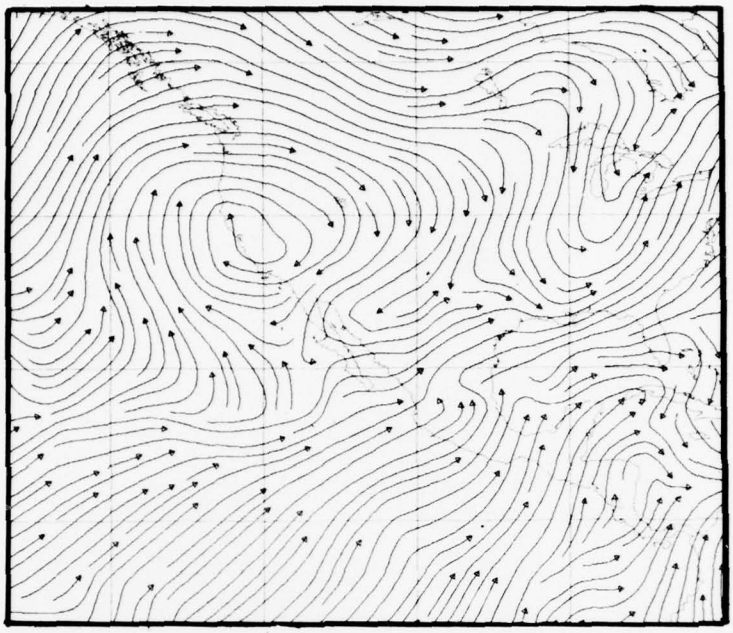

b. WIND-FIT

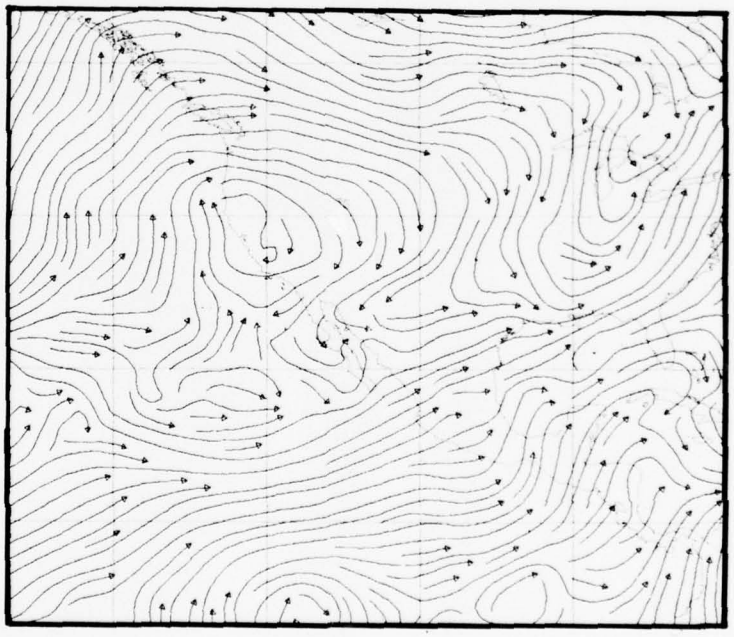

Figure 19. 300 mb streamline analyses, 00 GMT, 28 January 1976 for (a) Control, (b) Wind-fit, (c) Cloud-top, and (d) Cloud-base cases.

c. CLOUD-TOP

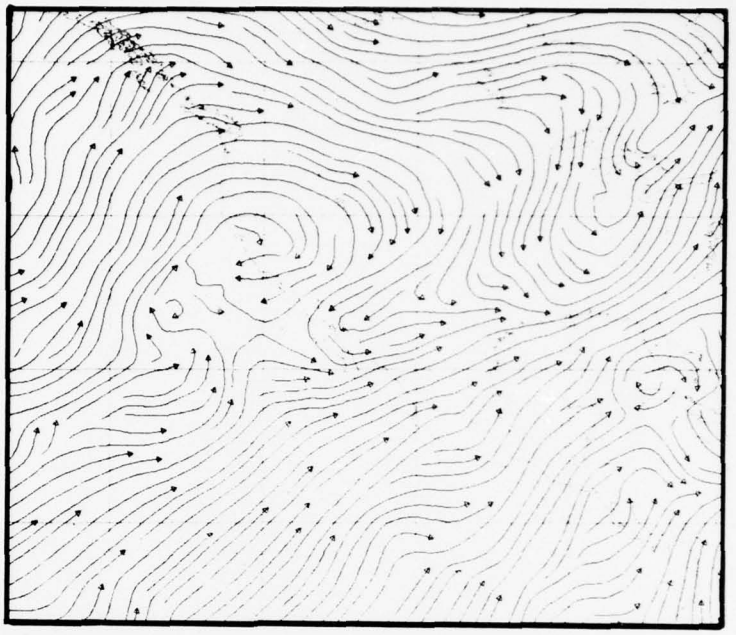

d. CLOUD-BASE

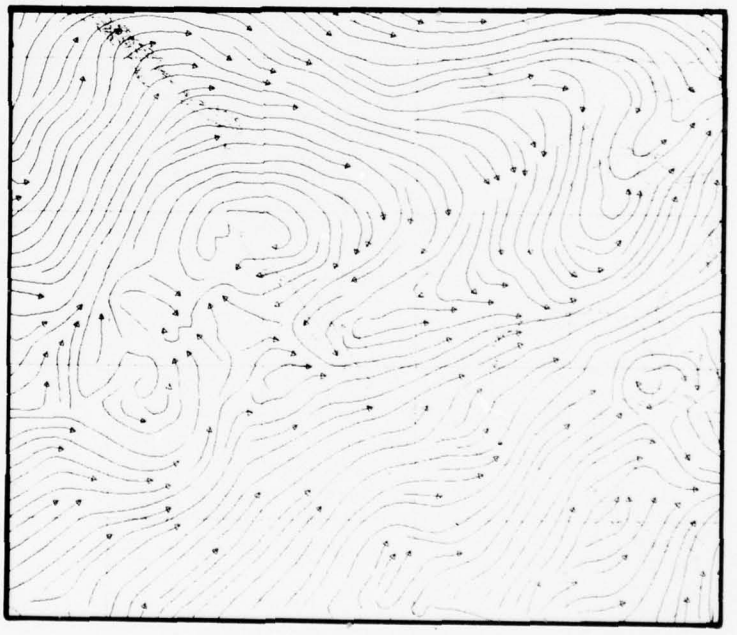

Figure 19. Continued.

a. CLOUD-TOP MINUS CONTROL

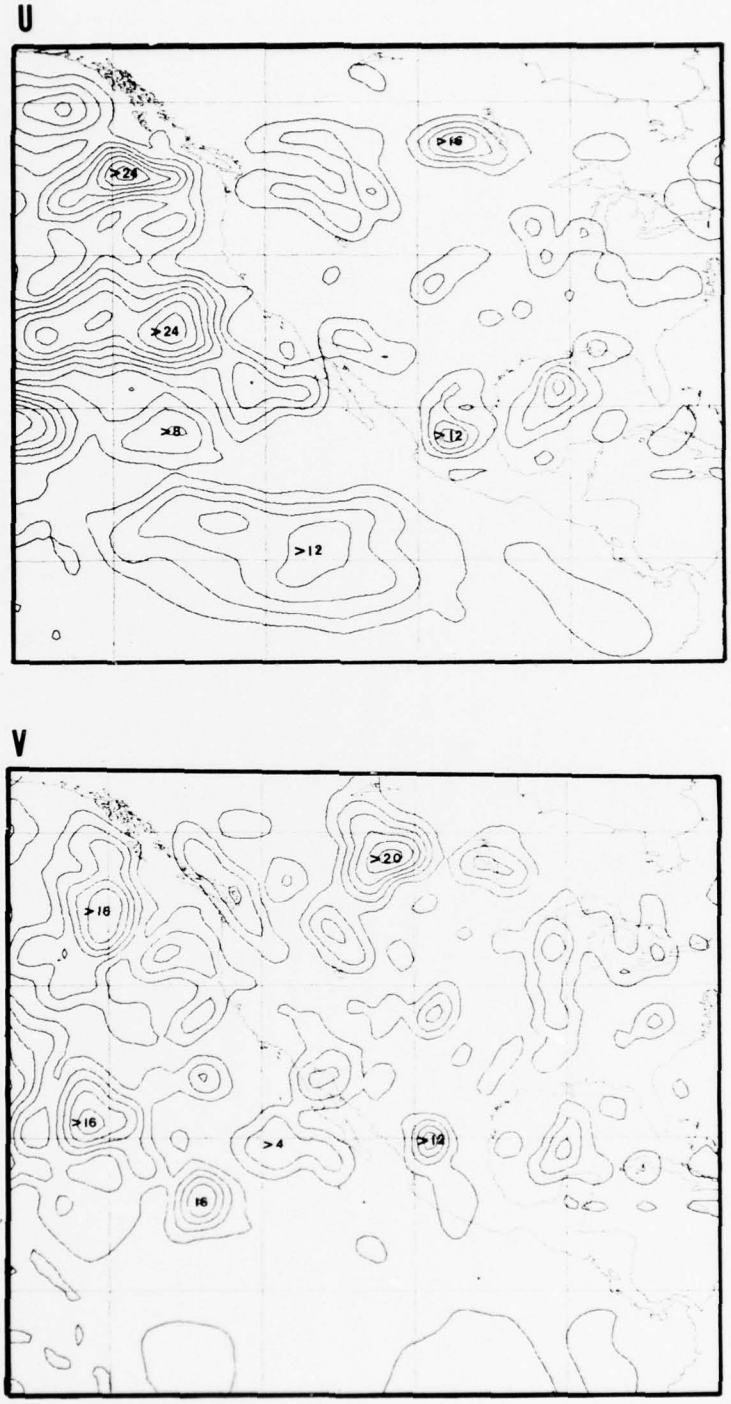

Figure 20. 250 mb root-mean-square wind differences between (a) Control and Cloud-top, (b) Control and Cloud-base, and (c) Control and Wind-fit cases. Both u- and v-components are shown with significant maximum and minimum values indicated in m/sec. The contour interval is 4 m/sec.

b. CLOUD-BASE MINUS CONTROL

U

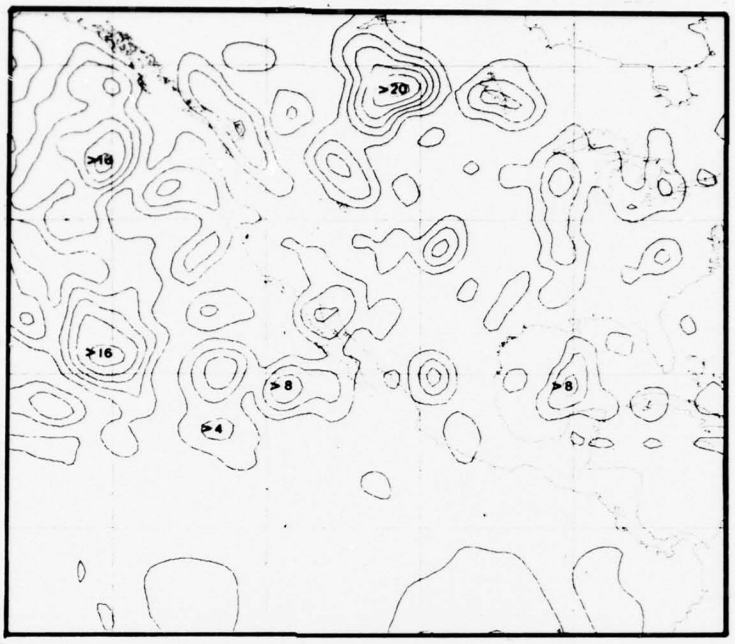

V

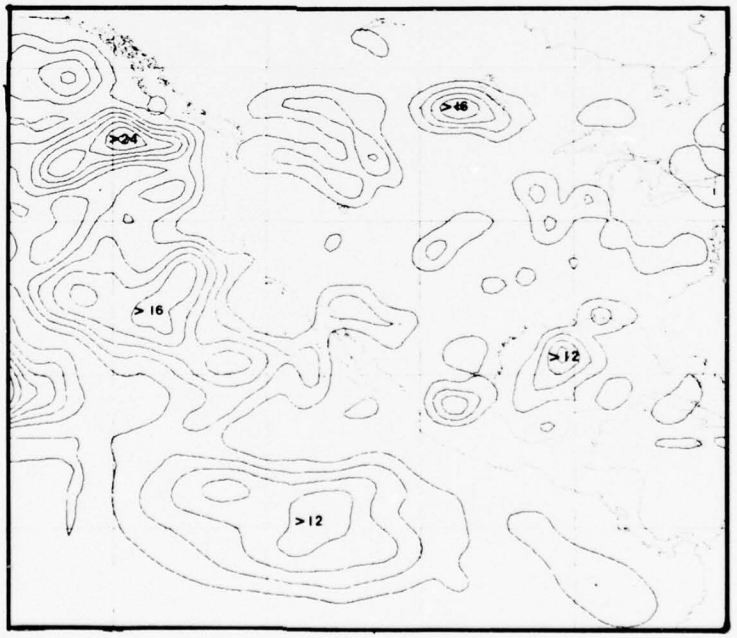

Figure 20. Continued.

c. WIND-FIT MINUS CONTROL

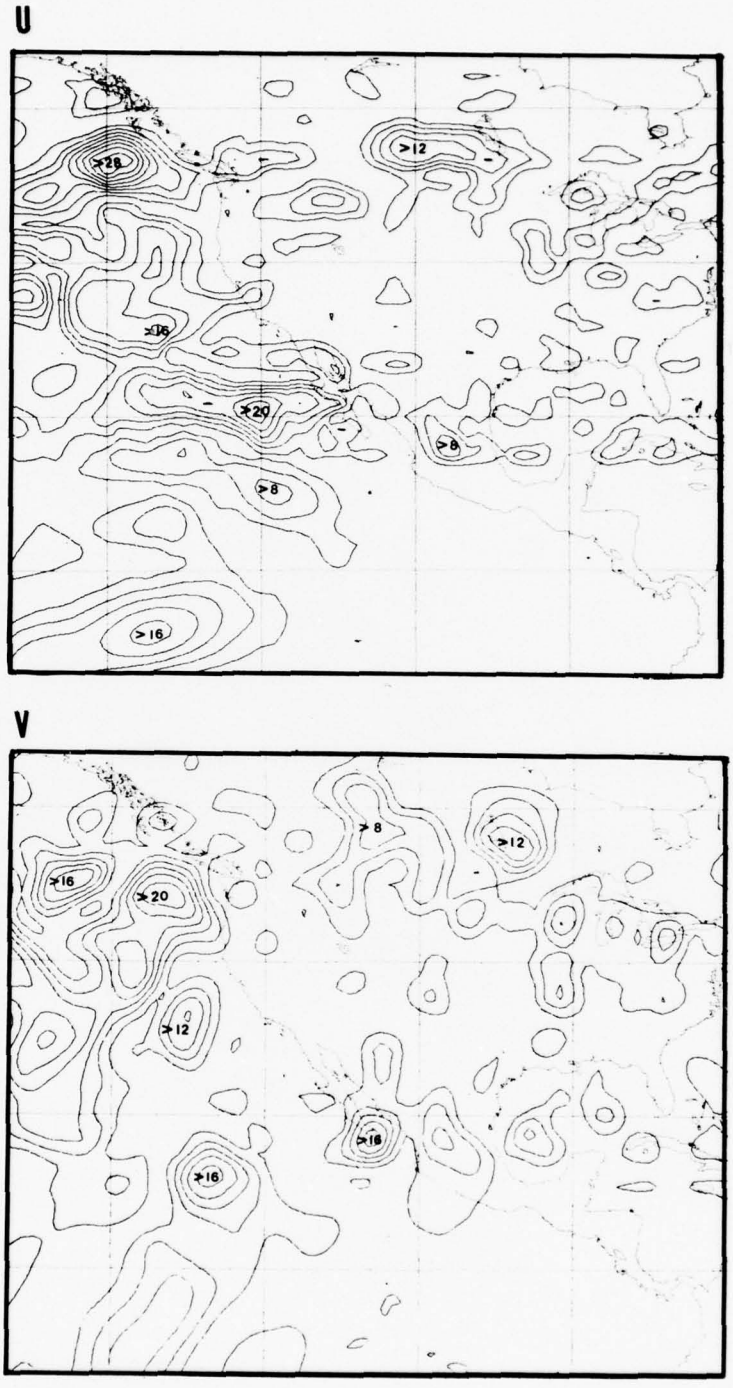

Figure 20. Continued.

The similarity between Cloud-base and Cloud-top cases noted in the streamlines (Figure 19) is still evident here. However, differences as large as 24 m/sec in the Cloud-top case and 16 m/sec in the Cloud-base case are apparent off the coast of California. These appear to be due to a large number of vectors which were inserted 12 hours previously at 250 mb by the Cloud-top method, but at 300 mb by the Cloud-base method, thus changing the structure of the trough west of this area. At the time these differences were computed, persistence had led to a difference of position of the trough and the extent of the high pressure area over California. Similar differences occur in the v-component RMS portrayal. It is not possible to state which result is the better of the two.

Despite the fact that the Wind-fit method fits the wind as closely as possible to the Control case, the RMS differences between the Wind-fit and Control cases after three days are larger in some areas than for the other two methods. This suggests that successive insertions agree with persistence to a larger extent in the temperature-based methods than in the Wind-fit method.

For 850 mb (Figure 21), the basic RMS differences between methods are as described above for 250 mb except that the overall RMS differences are not as great.

To investigate the temporal changes in the analyses, a mean value for each wind component over a specified area at each level for each time was computed, and a level versus time plot was constructed for each method and for Control. Means were computed and plotted for the tropics, the U.S., and an area of the Pacific. Diagrams for the ocean area, u-component, are shown in Figure 22. Area limits are from 50° to 20° north latitude and 145° to 125° west longitude. Note that the vertical coordinate, although labeled in pressure, has been plotted in height of the standard atmosphere at the pressure indicated.

The Cloud-top and Cloud-base cases are again very similar in their changes with time. Both portrayed the passage of the storm system through the area with maximum winds at 300 mb on 27 January at 00 GMT. However, the Cloud-top case decreased wind speeds in the area six hours slower than the Cloud-base case. Otherwise the differences are insignificant.

a. CLOUD-TOP MINUS CONTROL

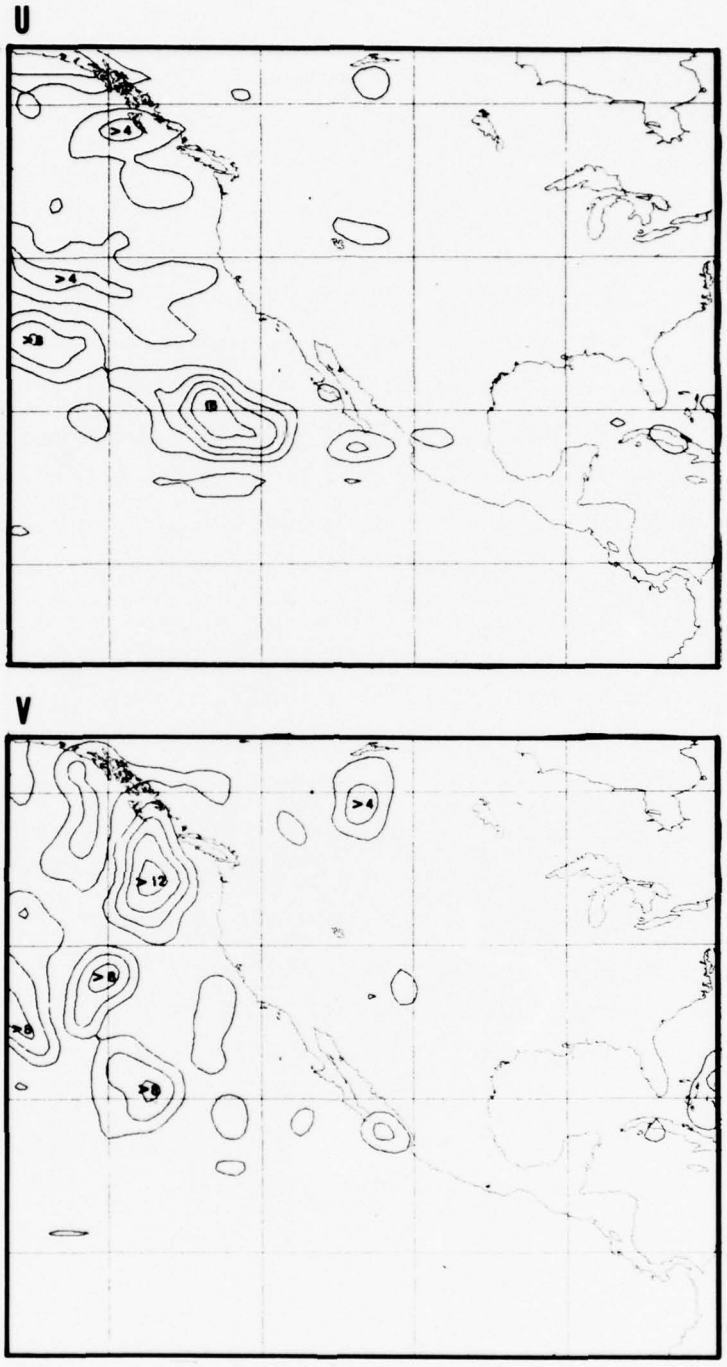

Figure 21. Same as Figure 20, but for 850 mb.

b. CLOUD-BASE MINUS CONTROL

U

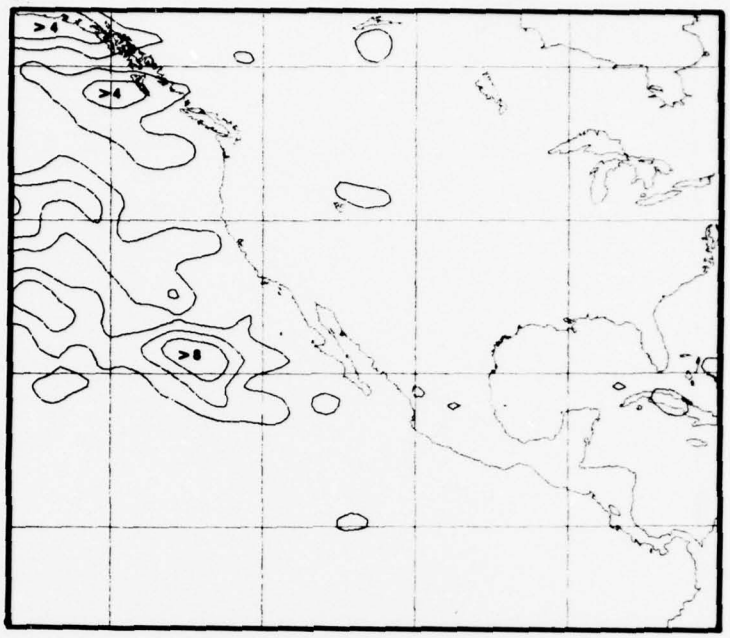

V

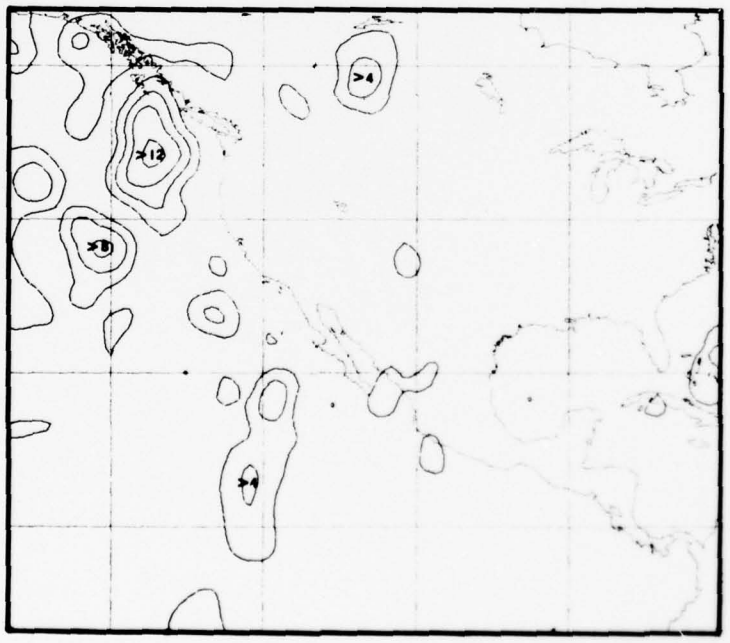

Figure 21. Continued.

c. WIND-FIT MINUS CONTROL

U

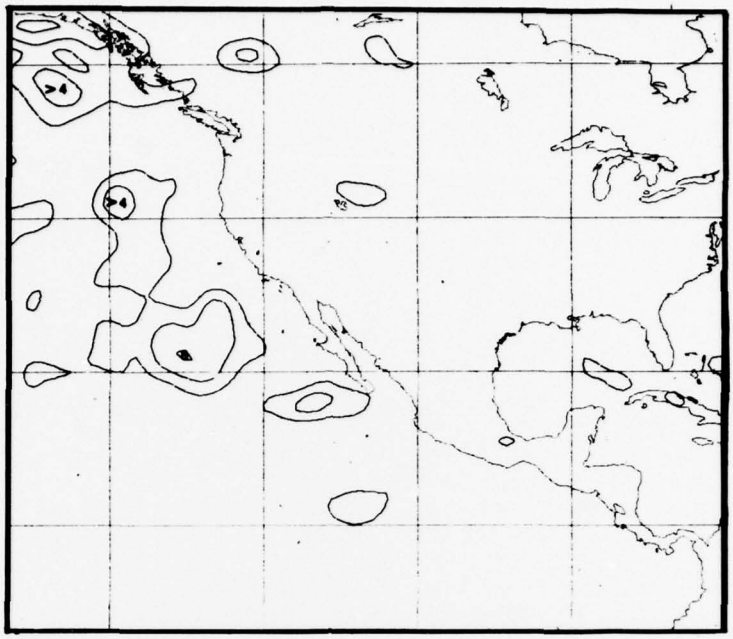

V

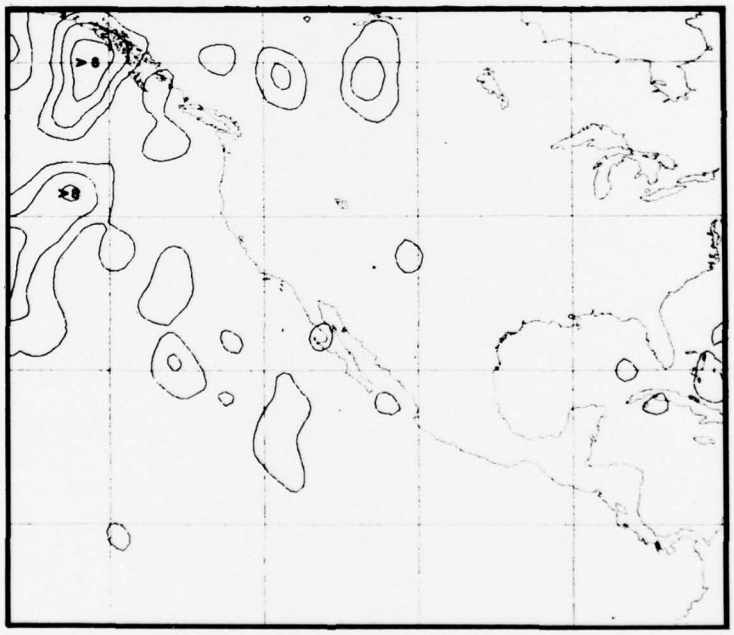

Figure 21. Continued.

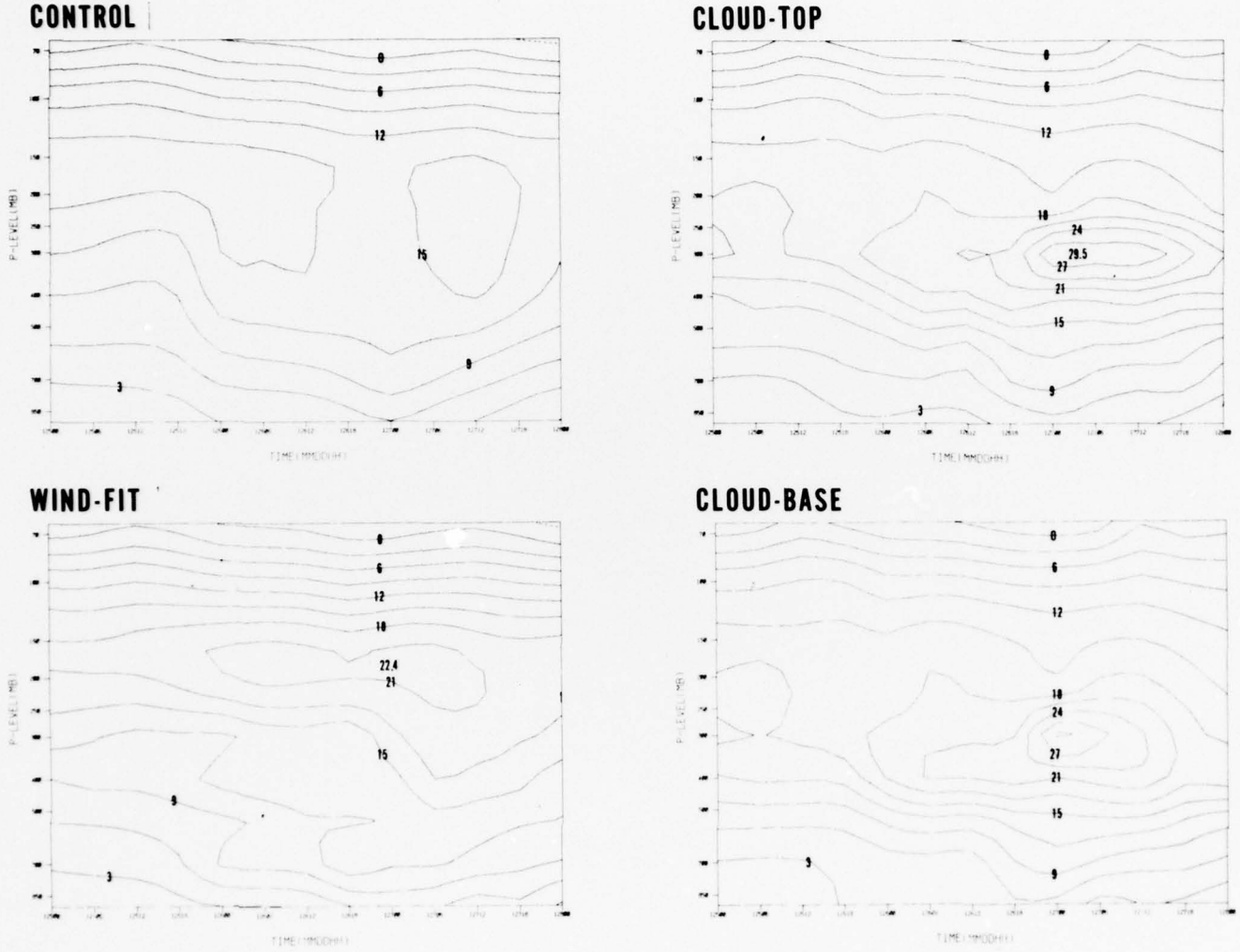

Figure 22. Temporal-vertical variation of the horizontal mean over an area of the Pacific Ocean of the u-component of the analyzed wind field. Area boundaries are 50°N to 20°N and 145°W to 125°W. Vertical coordinate is plotted in height of the Standard Atmosphere at the pressure indicated. Contour interval is 3 m/sec.

No identifiable wind maximum associated with the storm system in this area is seen in the Wind-fit or Control cases. This is reasonable for the Control result, given the lack of data in the area, but the same data available to the other two methods was available to the Wind-fit assimilation (only the level of insertion was changed). As shown previously, the Wind-fit method's characteristic of scattering tropopause vectors across five or more levels leads to minimal impact of the data at any one level. Interruptions in smooth changes such as those that occurred below 300 mb at 00 GMT and 18 GMT on 26 January are due to temporal inconsistencies in the CMV data such as the lack of definitive fleet boundaries.

Level-time analyses over the U.S. showed no differences as expected. In an area of the tropics, differences similar to those above were noted, although they were not as pronounced.

RMS wind differences at each level over a specific area between each of the three level determination methods and Control were computed for the last time of the experiments, 00 GMT, 28 January. Figures 23 and 24 are graphs of the u-component for two areas, a rawinsonde data-rich area and a rawinsonde data-sparse area, respectively. Latitude-longitude limits of the areas are 55°-25°N, 120°-170°W (Figure 23) and 25°N-5°S, 150°-100°W (Figure 24). All differences are nearly identical over the data-rich region with maximums at 70 mb and the tropopause. The Wind-fit curve gives lesser differences between 500 and 700 mb.

In the data-sparse region, there are greater differences between methods. Below 400 mb the Cloud-base case agrees best with the Control results. All three methods show large differences between 250 and 200 mb, although the Wind-fit case fares best. Above 150 mb the Cloud-base and Cloud-top cases yield identical RMS differences and are in slightly better agreement with the Control than the Wind-fit case. Overall, the Cloud-base method yields the best RMS differences in comparison to the Control case at the final analysis time.

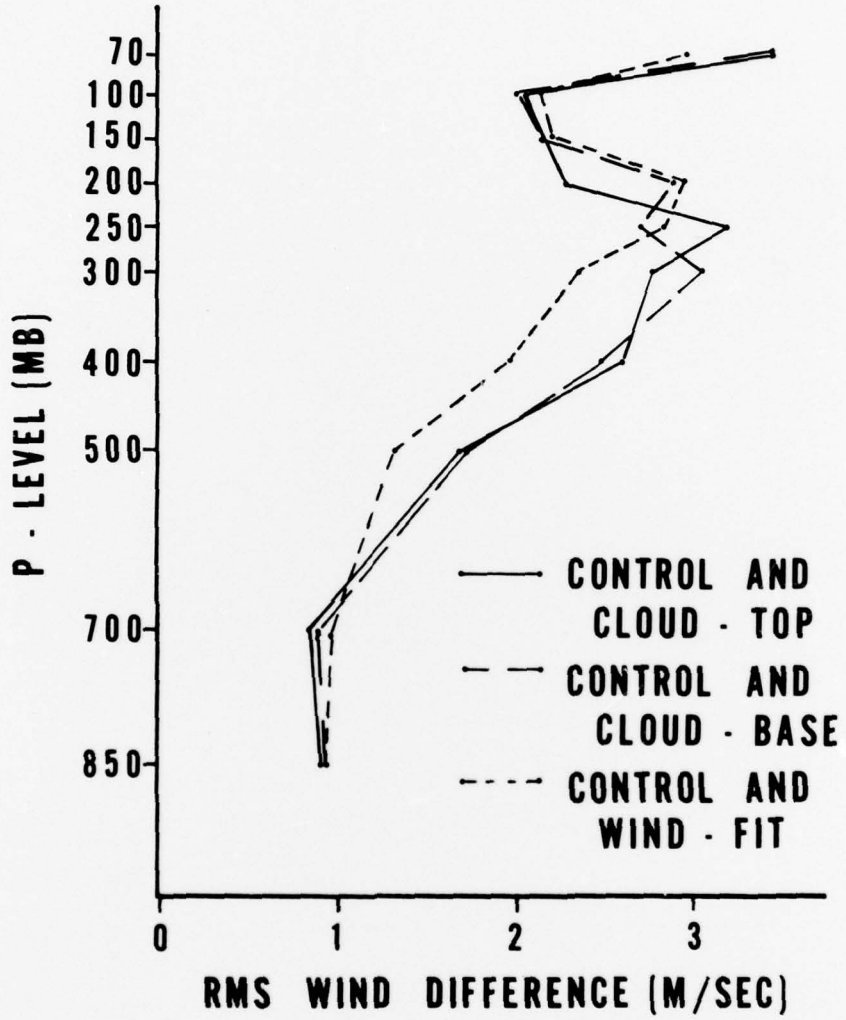

Figure 23. Vertical variation of the horizontal mean of the root-mean-square differences between Control and each of three cases for 00 GMT, 28 January 1976, for the u-component of the wind. Area is a rawinsonde-data-rich region with boundaries 55°-25°N, 120°-70°W.

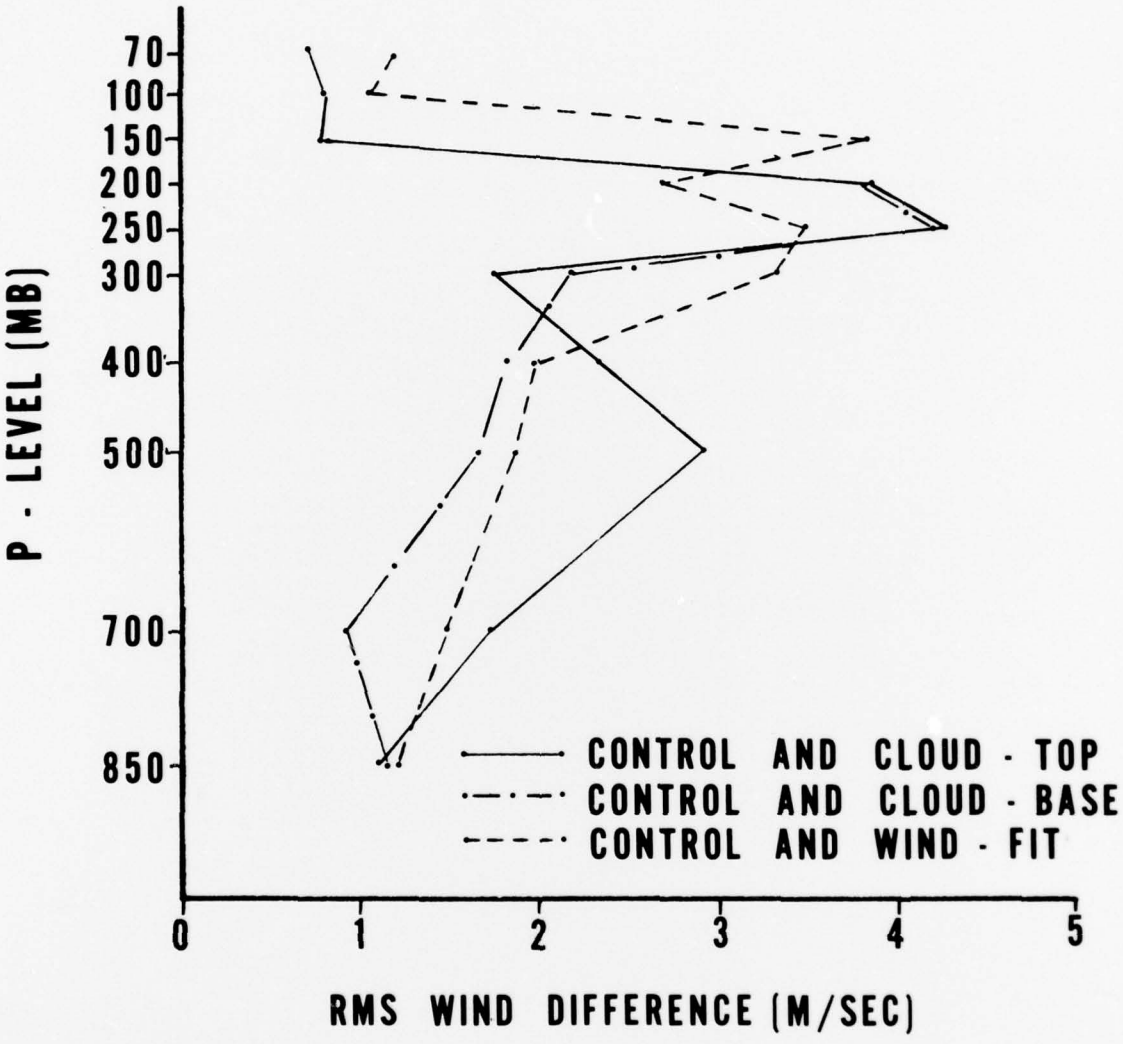

Figure 24. Same as Figure 23, but for a rawinsonde-data-sparse area with boundaries 25°N-5°S, 150°-100°W.

8. CONCLUSIONS

Due to the small influence of CMV in data-rich regions when combined with many rawinsonde observations, little effect on the analysis in any of the three level determination methods tested was noted in these areas. In regions sparse in rawinsonde data, however, CMV had a positive effect. The choice of method made only a slight difference in the analysis results after one cycle through the analysis, beginning with the same first guess. Rather, it was the effect of multiple insertions that led the analyses away from the Control case results and produced more meaningful analyses in the data-sparse areas. The use of persistence still gave reasonable analyses after three days of the analysis cycle.

The Cloud-top and Cloud-base methods showed very similar results, and from inspection of the one day of analyses using the Cloud-Inclusive method, it seems likely that it would have compared similarly. However, a number of results gave the Cloud-base case a slight edge over the other two if a choice was to be made: (1) Its vertical data distribution was the most realistic with respect to studies citing maximum numbers of vectors at 300 and 900 mb; (2) analysis results were in better agreement with individual original satellite images and image loops after three days; and (3) it demonstrated the overall best RMS wind difference in comparison to the control analysis for the final analysis results.

The Wind-fit method, by comparison, had characteristics and produced results that were questionable. The vertical distribution of the data was quantitatively uniform, and there was a tendency for the number of vectors at 850 mb and at 700 mb to converge over time till they were nearly equal. "Fleet" (p.16) boundaries were almost non-existent within the data after level determination, which caused vectors measured within the same cloud to be assimilated at different levels. Finally, the Wind-fit case had less effect on the analysis results, and in some instances a negative effect was evident.

As in all cloud motion vector studies, the lack of a definitive ground truth was a problem in these experiments. Comparisons with the first guess, satellite images and the Control case (a measure of the data's impact on the analysis), as well as comparisons of method results, were used to get a feel for the "most truthful."

One other general result was noted and deserves emphasis. The preservation of the identity of fleets of vectors appears to be important for enabling successive insertions to strengthen rather than negate the effect of previous insertions. Tentative data format specifications for the First GARP (Global Atmospheric Research Program) Global Experiment (FGGE) (GARP, 1978) allow for the specification of a fleet identifier which could be used to ensure that all vectors of a fleet are inserted at the same level.

9. CONTINUED EXPERIMENTATION

Because cloud motion vectors have proven their importance for use in numerical assimilation, it is necessary to continue experimentation to improve the quality and utilization of this information. Further study is particularly warranted in the problem area addressed in this study; the more accurate determination of insertion level. Assimilation with another type of objective analysis such as that developed by Barker (1978) is necessary to identify the effects of the statistical multivariate techniques within this study. A combination of the Cloud-base method in regions sparse in rawinsonde data and no CMV insertion in rawinsonde-data-rich areas should be tested, as should more sophisticated techniques such as level identification based on the known characteristics of a cloud's type. Forecast verification should be employed to fully gauge each method's accuracy.

Study regarding the fullest use of CMV in numerical assimilation is also necessary, realizing that the characteristics of these vectors are unique in comparison to other information sources. Two additional areas needing attention are determination of which quantity (vorticity, divergence, direction, etc.) is most useful, and identification of the special problems vertical coupling in assimilation may face when utilizing cloud-winds.

Much previous work in data assimilation has treated all input data the same. The best utilization of all data will result from combining each data source with each other source to extract the optimum information. Studies investigating the feasibility of computing wind profiles by coupling cloud motion vectors with satellite temperature soundings are of this persuasion. Also needed are advanced methods of blending GOES wind vectors with all types of conventional data.

The ultimate solution lies in the design of numerical model assimilation systems which take all data sources into account. The first step toward that end is the development of systems geared specifically to satellite data, beginning with the primitive

equations and building a model, basing each decision and choice in the development process on the characteristics of satellite data. The merging of this type of system with present, conventional-data-directed models could produce a unified system that truly uses all information.

ACKNOWLEDGMENTS

This research was carried out with the help and resources of three institutions: the University of Wisconsin (UW), the National Center for Atmospheric Research (NCAR), and the Naval Environmental Prediction Research Facility (NEPRF). Adaption of the objective analysis to this study, execution of the Control case, and offering of general guidance was by Dr. Thomas Schlatter, Mr. Grant Branstator, and Ms. Linda Thiel of NCAR. Dr. Verner Suomi and Mr. Fred Mosher at UW and Mr. Roland Nagle at NEPRF gave important suggestions. Finally, AG2 James Carlson, Mr. Dennis Daigle, Mr. Stephen Bishop, and Ms. Winona Carlisle helped with figures, photography, editing and typing, respectively.

REFERENCES

Barker, E., 1978: Personal communication.

Bengtsson, L., and P. Morel, 1974: The performance of space observing systems for the first GARP global experiment. GARP Working Group on Numerical Experimentation, Rept. No. 6, 23 pp.

Bengtsson, L., 1975: Four-dimensional assimilation of meteorological data. GARP Publication Series No. 15, WMO/ICSU, 76 pp.

Chatters, G. C., and V. E. Suomi, 1975: The applications of McIDAS. IEEE Transactions on Geoscience Electronics, GE-13, (3), 137-146.

Chatters, G. C., 1976: The satellite image wind system. Proc. Symp. Met. Observ. from Space: Their contribution to the FGGE, 195-197.

Davis, P. A., R. G. Hadfield, and E. J. Wiegman, 1973: Infrared emissivities and upper-tropospheric cloud motions. Final rept., Contract 2-37131, Stanford Research Institute, Menlo Park, CA, 55 pp.

Davis, P. A., 1976: Height positioning of cloud-motion vectors from satellite infrared tracking over GATE area. Final rept., Contract No. 5-35444, Stanford Research Institute, Menlo Park, CA, 58 pp.

Fujita, T. T., D. L. Bradbury, C. Murino, and L. Hull, 1968: A study of mesoscale cloud motions computed from ATS-1 and terrestrial photographs. Satellite and Mesometeorology Research Project Rept. No. 71, Univ. of Chicago, 25 pp.

Fujita, T. T., E. W. Pearl, and W. E. Shenk, 1975: Satellite-tracked cumulus velocities. J. Appl. Meteor., 14, 407-413.

Gandin, L. S., 1963: Objective analysis of meteorological fields. Gidrometeorologicheskoe Izdatel'stvo, Leningrad. Translated from Russian, Israel Program for Scientific Translations, Jerusalem, 1965, 242 pp.

Global Atmosphere Research Program, 1978: Report on Informal FGGE Quality Control Meeting, Univ. of Wisconsin, Jan 10-12, 19 pp.

Hasler, Arthur, 1972: Properties of tropical cloud clusters determined from geostationary satellite pictures. Ph.D thesis, Univ. of Wisconsin, 317 pp.

Hasler, A. F., and W. E. Shenk, 1977: Wind estimates from cloud motions: Results of an in situ aircraft verification experiment. National Aeronautics and Space Administration (NASA) Weather and Climate Program Science Review, NASA Conf. pub., 20-29.

Hasler, A. F., W. E. Shenk, and W. C. Skillman, 1977: Wind estimates from cloud motions: Results from Phases I, II, and III of an in situ aircraft verification experiment. J. Appl. Meteor., 16, 812-815.

Hayden, C., 1973: Experiments in the four-dimensional assimilation of Nimbus 4 SIRS data. J. Appl. Meteor., 12, 425-435.

Hubert, L. F., 1976a: The relation between cloud pattern motion and wind shear. Mon. Wea. Rev., 104, 1167-1171.

Hubert, L. F., 1976b: Wind determination from geostationary satellites. Proc. Symp. Met. Observ. from Space: Their contribution to the FGGE, 211-213.

Hubert, L. F., and L. F. Whitney, Jr., 1971: Wind estimation from geostationary satellite pictures. Mon. Wea. Rev., 99, 665-672.

Lemar, P., and W. Bonner, 1975: Study report on satellite winds: Comparisons between NESS and Wisconsin cloud-tracked winds. NMC Data Assimilation Branch, Development Division, NASA Contract S-70252-AG, 23 pp.

Miyakoda, K., L. Umscheid, D. H. Lee, J. Sirutis, R. Lusen, and F. Pratte, 1975: The near real time global four-dimensional analysis experiment during the GATE period, part I. J. Atmos. Sci., 33, 561-531.

Mosher, F., 1974: SMS cloud heights. Space Science Engineering Center rept., Univ. of Wisconsin, 25 pp.

Mosher, F. R., 1976a: Cloud height determination. Proc. Symp. Met. Observ. from Space: Their contribution to the FGGE, 201-204.

Mosher, F. R., 1976b: Report on the Wisconsin participation in the January-February 1976 DST report on NASA Contract NAS5-23296, Space Science and Engineering Center, Univ. of Wisconsin.

Otto-Bliesner, B., D. P. Baumhefner, and T. W. Schlatter, 1977: A comparison of several meteorological analysis schemes over a data-rich region. Mon. Wea. Rev., 104, 1083-1091.

Schlatter, T. W., 1975: Some experiments with a multivariate statistical objective analysis scheme. Mon. Wea. Rev., 103 246-257.

Schlatter, T. W., G. W. Branstator, and L. G. Thiel, 1976: Testing a global multivariate statistical objective analysis scheme with observed data. Mon. Wea. Rev., 104, 765-783.

Schlatter, T. W., 1977: Personal communication.

Smith, E. A., 1975: The McIDAS system. IEEE Transactions on Geoscience Electronics, GE-13 (3), 123-136.

Smith, C. L., and A. F. Hasler, 1976: A comparison of low-cloud satellite wind estimates with analyses based on aircraft observations in a disturbed tropical regime. Mon. Wea. Rev., 104, 702-708.

Suchman, D., D. W. Martin, F. R. Mosher, B. Sawyer, and K. G. Bauer, 1975: Preliminary assessment of the cloud tracking system development at the University of Wisconsin. Space Science and Engineering Center rept., Univ. of Wisconsin, 77 pp.

Suomi, V. E., 1975: Man-computer interactive data access system (McIDAS): Continued development of McIDAS and operation in the GARP Atlantic tropical experiment. Final rept., Contract NAS5-23296, SSEC, Univ. of Wisconsin, 255 p.

Viezee, W., D. E. Wolf, and R. M. Endlich, 1977: Evaluation of the FIB methodology for application to cloud motion wind data. Final rept., Contract N00228-76-C-3182, Stanford Research Institute, Menlo Park, CA, 92 pp.

Young, J. T., 1976: Navigation of geostationary images. Proc. Symp. Met. Observ. from Space: Their contribution to the FGGE, 198-200.

APPENDIX A

ANALYSIS FIRST GUESS

A.1 PERSISTENCE AND CLIMATOLOGY

Each analysis cycle used both persistence and a climatology as first guesses in different parts of the grid. If the grid point being analyzed was at a location outside the tropics (greater than 20° latitude), persistence was used as a first guess for all data points within the 1500 km range used to calculate the grid point value. For all grid points in the tropics, climatology was used. Since a grid point could be at 15°N but might use a data point at 28°N, an overlap was needed. Thus, persistence was utilized between 75°N and 5°N and climatology was used between 35°N and 15°S.

A.2 INITIAL FIRST GUESS FOR PERSISTENCE

For temperature, the initial first guess for persistence was the National Meteorological Center (NMC) operational analysis for the initial time, 00 GMT on 25 January, 1976. Unfortunately, this analysis was available only between 18°N and 75°N. All points at the equator were set equal to the mean of all points in the row at 18°, and then rows between 5°N and 18°N were linearly interpolated.

For the wind, the initial first guess was geostrophically computed from a height field with the Coriolis parameter for 20° used for latitudes less than 20°. The height field was the NMC analysis with interpolation to 5°N as was done for temperature.

A.3 CLIMATOLOGY

A winter set of climatology values was available for this grid for the u and v components of the wind, but not for temperature. Instead, an ersatz climatology was assumed by using the above-defined persistence first guess to 5°N, continuing the interpolation to the equator, and assuming a uniform field south of the equator equal to the value at the equator. This was a poor first guess, but it was generated by NCAR without control of the author. Height was not analyzed in the tropics, so no climatology was needed.